Eidgenössische Technische Hochschule Zürich
Swiss Federal Institute of Technology Zurich

Architecture and Building Systems

Michiel Jansen

Life Cycle Assessment of New Building Technologies: HiLo Project

Master Thesis

ITA – Architecture and Building Systems
Swiss Federal Institute of Technology (ETH) Zurich

Examiner:
Prof. Dr. Arno Schlüter

Supervisors:
Prageeth Jayathissa, Niko Heeren

Zurich, November 3, 2015

We shape our buildings,
thereafter they shape us.

WINSTON CHURCHILL

Abstract

Acknowledgement

Contents

List of acronyms

AP	Acidification Potential
ASF	Adaptive Solar Facade
BOS	Balance of System
DA	Deplation Abiotic Resource
DAC	Disposal Acidification Coefficient
DCC	Disposal Carbon Coefficient
DEC	Disposal Energy Coefficient
E	Eutrophication
EAC	Embodied Acidification Coefficient
EC	Embodied Carbon
ECC	Embodied Carbon Coefficient
EE	Embodied Energy
EEC	Embodied Energy Coefficient
EOL	End Of Life
EPBT	Energy Pay Back Time
FT	Freshwater eco-toxicity
GER	Gross Energy Requirement
GWP	Global Warming Potential
HT	Human Toxicity
ICE	Inventory on Carbon and Emissions
IEA	International Energy Agency
IPCC	Intergovernmental Panel on Climate Change
ISO	International Organization for Standards
LCA	Life Cycle Assessment
LCI	Life Cycle Inventory
OE	Operational Energy
SMQ	Specific Material Quantity
UNEP	United Nations Environmental Program
W	Waste Creation
WBCSD	World Business Council for Sustainable Development

List of Figures

List of Tables

Chapter 1

Introduction

1.1 Motivation and literature review

In the last decade, environmental problems related to energy use and supply, such as climate change, water scarcity and acidification, became increasingly important. The increasing general awareness that there are limits to the abundance of non-renewable resources and limits to regulating ecosystem services, made sustainability a global issue[17]. The solution to these problems involves the rational use and supply of (non)renewable resources and reducing the emission of pollutants[18][19]. Due to the growth in global primary energy use and the ambition to move to less CO_2 intensive energy resources due to climate change, energy efficiency and CO_2 emission reduction are the most economical and most important options to mitigate climate change according to the Fifth Assessment Report of the Intergovernmental Panel on Climate Change (IPCC)[20].

Roughly 40% percent of global primary energy consumption and 30% of CO_2 emissions originate from buildings according to the United Nations Environment Program (UNEP)[21]. This is a higher proportion for both primary energy consumption and emissions than any other sector[22]. Because of this, buildings are important for the reduction of energy demand and CO_2 emissions. The building sector was identified by Pacala and Socolow as one of the "seven stabilization wedges that could help balance the growth in CO_2 emissions in the next 50 years"[23]. This potential was also identified by the World Business Council for Sustainable Development (WBCSD), which concluded that the energy use of buildings could be reduced by up to 60% worldwide in a cost effective manner[24]. Furthermore, McKinsey & Company stated in their research that emission reduction in the building sector would be the most cost effective measure with a negative cost for CO_2 abatement, when looking at cost curves in all sectors of the economy[25].

For the assessment of the environmental impact of buildings or products a wide range of methods/metrics exists[26][27]. A way to have consistency in these metrics is the use of an international standard for the determination of the environmental impact[28]. This is why the International Organization for Standards (ISO) created standard guidelines, the ISO 14040 and ISO 14044. One of the methods, which is based on these guidelines, is Life Cycle Assessment (LCA)[29]. LCA quantifies the environmental impact of processes and goods over their entire lifetime from "cradle" to "grave"[30]. The international consensus of the definition of LCA is:"compilation and evaluation of the inputs, outputs, and potential environmental impacts of a product system throughout its life cycle"[6]. LCA is a widely used decision support tool in industry and government, as it allows the analysis and optimization of the environmental impact and helps pin-point crucial areas in complex decision making or design.

Research on LCA in the building sector is less developed than in other sectors like for example waste management, however it is quickly developing and already widely used in the building industry[31][32]. Many LCAs have been made by consulants, architects and engineers to evaluate buildings [33] or even entire urban areas[34][35]. Currently LCA is limited to environmental impacts, however efforts have been undertaken to include social and economic dimensions of sustainability[36] and the creation of life cycle cost analyses[37], but these are out of the scope of this thesis.

LCA holds several impact categories, which can be evaluated. The three types of impact categories where determined based on relevance to the LCA framework [29]: baseline categories, study-specific impact categories and other impact categories. Within these categories there are various variables, which can be calculated. The research in this thesis will mainly focus one key variable: emissions of CO_2 equivalent (CO_2eq), which falls under the baseline category. CO_2eq is the weighted greenhouse gas emissions to an equivalent amount of CO_2, as for example methane is a much worse greenhouse gas than carbon itself. Broad consensus has been reached on this variable for both the data and methodology [38]. Next to this, the scope of the thesis will be extended to the baseline categories: acidification, life cycle energy and energy pay-back time, when relevant.

Emissions of CO_2eq occur over the entire lifetime of the building e.g. from the chemical processes of manufacturing concrete to the operational use of air-conditioning. Furthermore, the focus of this thesis will be on three aspects of the life cycle assessment of CO_2eq:

- Embodied carbon: emissions due to material use for construction and construction processes
- Operational carbon: emissions due to heating, cooling, ventilation, hot water and lighting
- Disposal carbon : emissions due to disposal of materials and processes to dispose the building

This thesis will focus on these three aspects for several reasons. First, research in the field of embodied carbon is underdeveloped and this thesis can therefore contribute to the further understanding of embodied carbon[39]. Second, the breakdown into these three aspects helps pinpoint and elaborate on the relationship between embodied carbon and operational carbon[40]. This relationship becomes of increasing importance, as more sustainable buildings are being built, which require higher material use, therefore increasing the share of embodied carbon in relation to the total LCA. Also, because of this, lifetime of the building or building technologies becomes important, when buildings or technologies are disposed with a short life cycle, the proportion of embodied and disposal carbon becomes bigger in relation to operational carbon. Last, literature on the relationship between embodied and operational vary widely for both energy and carbon. For embodied energy Adalberth mentions in his case studies that 80-90% of total energy comes from operational energy, while 10-20% comes from embodied energy and a negligible amount from disposal[41]. Cole and Kernan report 4-9% for embodied energy[42], while Webster shows 2-20% for embodied energy [43]. Thormak reports that this relationship changes significantly due to the difference in high and low energy buildings, where newer buildings are shifting more and more towards embodied energy[44], which is also confirmed by Santori and Hestnes.

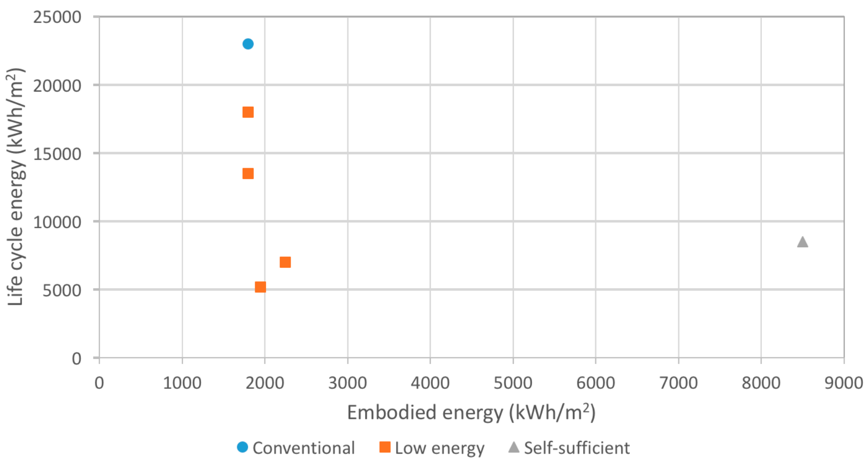

Figure 1.1: Embodied energy in relation to life cycle energy[1]

Sartori and Hestnes looked at case studies of conventional buildings, low energy buildings and self-sufficient buildings in the residential sector and came to the conclusion that embodied energy reduction becomes very important for low energy and self-sufficient buildings, as shown in Figure 1.1[1]. It can be seen that reducing operational energy is possible untill a certain point, where embodied energy becomes the most important factor. Therefore reduction optimization for embodied energy should not be neglected, as considerable savings can be realized. Reddy and Jagadis show a 30-45% reduction in embodied energy for residential buildings[45].

Next to the type of building (conventional, low energy, self sufficient), embodied energy also greatly depends on construction type and materials used. Figure 1.2 shows the embodied energy of a 8-storey residential building in Melbourne using: conventional concrete, prefabricated steel and prefabricated timber[2]. It can be seen that prefabricated concrete outperforms both steel and timber constructions for embodied as well as operational energy.

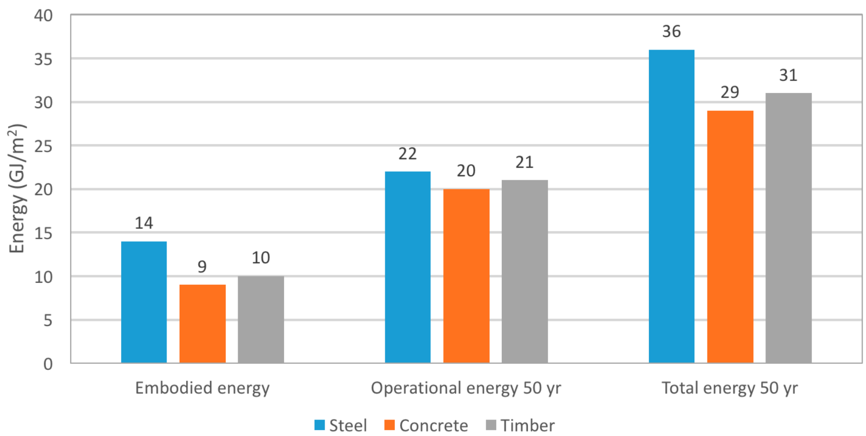

Figure 1.2: LCA three construction types[2]

The share of embodied carbon in relation to total carbon is even higher than embodied energy, however figures vary also here significantly. The range for embodied carbon lies between 11-80% according to Simpson[46]. De Wolf created an overview of embodied carbon (EC) and embodied energy (EE) ranges, which can be seen in Figure 1.3. Cole & Kernan[42] show a range for embodied energy between 4-9% , Eaton & Amato[32] show 37-43% for embodied carbon, Build Carbon Neutral[47] estimates the share of embodied carbon between 13-18%, Simpson[46] states the share of embodied carbon up to 80%, Athena[48] reports 9-12% share for embodied energy, Arup[49] states a 11-50% share of embodied carbon and Webster[43] reports a range of 2-22% for embodied energy.

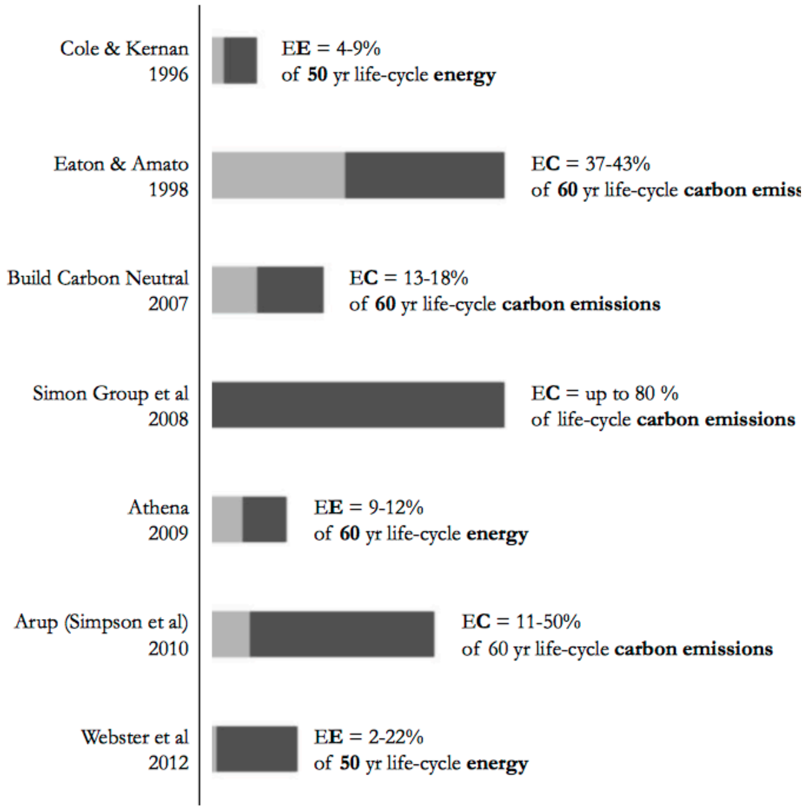

Figure 1.3: Ranges of embodied carbon and embodied energy[3]

This thesis will mainly focus on applying a life cycle analysis of embodied, operational and disposal carbon, as described above, to the adaptive solar facade (ASF), thin-shell roof and funicular floor for the HiLo building project in Zurich, Switzerland developed by the Institute of Technology in Architecture of ETH Zurich. These concepts are new building technologies currently under development, which try to decrease operational carbon (ASF), embodied carbon (funicular floor) or total carbon (roof) to advance the sustainability of buildings. This thesis therefore tries to quantify the carbon reduction of these technologies to fill in the knowledge gap on these technologies and advance the understanding of both embodied carbon and operational carbon in the design of buildings.

The adaptive solar facade is part of the building envelope, which acts as buffer between the interior and exterior environment. The ASF combines passive methods, such as shading[50][51], natural daylight distribution[52] and a heat dissipative construction[53] together with active solar energy harvesting via photovoltaic panels[54] to decrease operational energy needs and operational carbon emissions of the building[14]. The ASF comprises of a frame with an array of individually actuated solar panels attached to the facade of a building, as seen in Figure 1.4. This allows the ASF to create a dynamic optimal mix between daylight distribution, direct radiation and producing electricity[14]. The panels are actuated using soft pneumatic robotics[55], which allows for more durability and reduces mechanical stress due to wind. Next to this, the ASF facilitates new aesthetic kinetic architectural design, mentioned by Fortmeyer[56] and Giselbrecht[57].

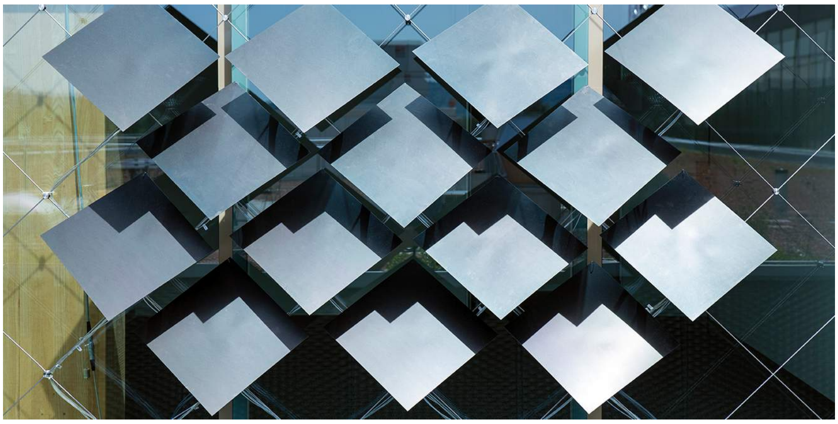

Figure 1.4: Impression of the adaptive solar facade[4]

The thin-shell roof consists out of a very lightweight and thin sandwich structure with thin-film photovoltaic solar cells on the top layer[58].The surface area of the roof is also used for heat transfer into the building using hydronic cooling and heating. The shape of the roof is designed using multi-objective evolutionary shape optimization.

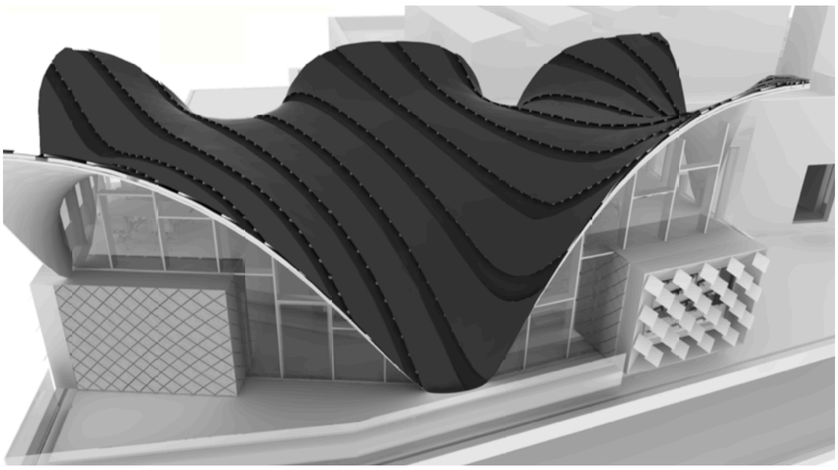

Figure 1.5: Impression of the thin-shell roof[5]

The funicular floor is a prefabricated lightweight concrete floor structure with 70% less mass than conventional concrete floor slabs. Therefore reducing embodied carbon significantly, as less material is used[59].

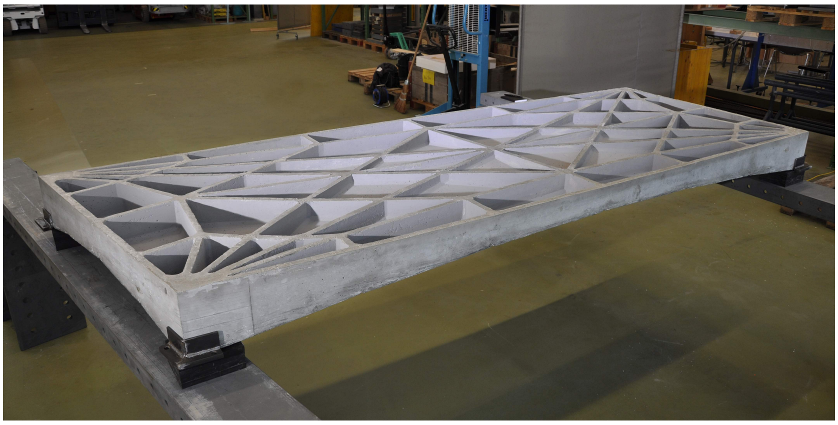

Figure 1.6: Impression of the funicular floor[5]

1.2 Research objective

The goal of the thesis is to quantify the operational, embodied and disposal carbon and other environmental impact parameters, such as energy and acidification potential, for the new innovative techniques used in the HiLo building. This will drive insight in the performance of the new technologies, as well as fill the knowledge gap on the relationship between embodied and operational carbon in building design.

First, the thesis will start with the assessment of the adaptive solar facade. This leads for example to the insight which components are most carbon intensive and how much life cycle carbon does the solar facade hold relative to standard (comparable) systems/technology. Both the insight in carbon intensive components (embodied or operational) and the total emissions relative to other technologies can then drive new design considerations for the system.

Also, this approach is then applied to the thin-shell roof (including insulation, thin-film PV etc.) and the funicular floor system to give an insight in all new technologies used in the HiLo building.

1.3 Thesis outline

Chapter 2 discusses the methodology and the life cycle assessment in detail, addressing an overview on the methodology and scope of the assessment, definition of concepts used and explanation of assessment tools and databases.

Second, Chapter 3 assesses the three case studies of the adaptive solar facade, thin-shell roof and funicular floor, compares the technologies with conventional technologies and gives design considerations.

Last, Chapter 4 summarizes the conclusions, discusses the key contributions of the thesis and gives an outlook on future research.

Chapter 2

Methodology

The methodology for the life cycle analysis of the technologies of the HiLo project is based on the international standards: ISO14040 and ISO14044, as discussed in Chapter 1. This Chapter will first give a general overview on the LCA methodology and the 4 stages of an LCA. Subsequently the first stage of the LCA (goal and scope definition) is fully discussed in this Chapter, as it is part of the methodology. Next, the databases and tools used for stage 2 (inventory analysis) and stage 3 (impact assessment), are discussed. The calculations and results of stage 2 and stage 3 together with the last stage (interpretation) are discussed during the survey of technologies in Chapter 3.

2.1 Overview of general LCA methodology

The four steps of a life cycle analysis, as given in literature, are[33]:

1. **Goal and scope definition** determines the impact categories together with their functional unit, system boundaries and quality criteria for inventory data

2. **Inventory analysis** collects the inventory data and determines the use of databases

3. **Impact assessment** calculates the final life cycle impact categories based on the data

4. **Interpretation** of results from both the inventory analysis and impact assessment

These four stages interact with each other, for example changing the scope will change the inventory analysis, as other data will be required. This, in turn, will then influence the final impact assessment. The interpretation stage interacts with all stages, as the choice of category, specified in the first stage, or the choice of inventory data, specified in the second stage, or the choice of calculation method can depend on how definitions and results are interpreted in the end. These interactions are visible in the diagram of the LCA framework in Figure 2.1.

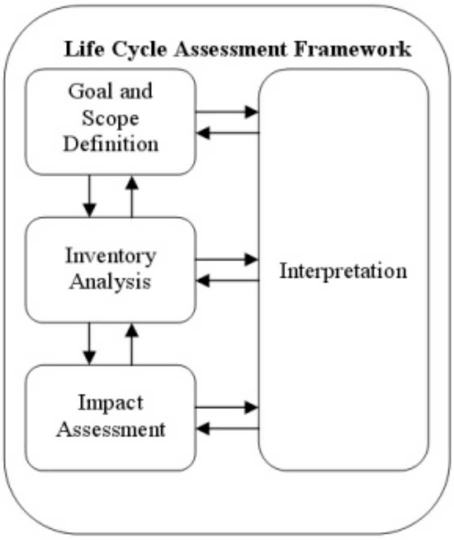

Figure 2.1: LCA framework based on ISO14040[6]

2.2 Goal and scope definition

The goal of the life cycle assessment is the evaluation, relative performance and optimization of the adaptive solar facade, thin-shell roof and funicular floor. The main impact category, which will be used as optimizing and comparison variable, is the emissions of CO_2eq divided by the functional unit, as discussed in Chapter 1. Additional categories will be added based on environmental relevance to the technology.

2.2.1 Impact categories and functional unit

For the three different technologies, four impact categories will be evaluated: global warming potential, gross energy requirement, energy pay back time and acidification potential. These categories are most relevant to the technologies and most widely used in existing literature on life cycle assessment according to Ortiz et al.[16]. Table 2.1 gives an overview of published case studies in the build environment and the incorporated impact factors.

Table 2.1: Published LCA impact factors considered in case studies within the building sector[16]

Reference	GWP	AP	E	HT	GER	DA	W	FT
Adalberth et al.[60]	✓	✓	✓	✓	✓			
Ardente et al.[61]							✓	
Arena & Rosa[62]	✓		✓		✓			
Asif et al.[63]	✓							
Citherlet et al.[64]	✓	✓						
Jian et al.[65]	✓				✓		✓	
Junnila[66]	✓	✓	✓		✓			
Koroneos & Dompros[67]	✓	✓	✓				✓	
Koroneos & Kottas[68]	✓	✓	✓		✓			
Nebel et al.[69]	✓	✓	✓					
Nicoletti et al.[70]	✓	✓		✓		✓		
Nyman and Simonson[71]	✓	✓				✓		
Peuportier[72]	✓	✓	✓	✓	✓	✓	✓	✓
Petersen & Solberg[73]		✓	✓	✓				
Prek[74]	✓							
Ross & Evans[75]							✓	
Saiz et al.[76]	✓	✓	✓	✓			✓	
Scheuer et al.[31]	✓	✓			✓		✓	
Schleisner[77]					✓			
Seppala et al.[78]			✓	✓	✓		✓	
Wu[79]	✓	✓	✓		✓			
Total	**16**	**13**	**11**	**6**	**10**	**3**	**8**	**1**

Abbr. respectively: global warming potential, acidification potential, eutrophication, human toxicity, gross energy requirement, depletion abiotic resource, waste creation and freshwater eco-toxicity.

As can be seen, global warming potential, acidification potential and gross energy requirement are mostly used. Furthermore, based on the motivation of this thesis, the relationship between embodied and operational carbon for the global warming potential would fill a big knowledge gap in literature, as discussed in Chapter 1. For the adaptive solar facade, energy pay back time is also added, as most reviews on photovoltaic panels include the energy pay back time [80][8], however it is not an official impact factor according the the LCA handbook and is calculated separately as a result of this. Table 2.2 gives an overview of the categories evaluated per technology for this thesis.

Table 2.2: Overview of impact categories per building technology

Categories	ASF	Thin-shell roof	Funicular floor
Global warming potential (GWP)	✓	✓	✓
Gross energy requirement (GER)	✓	✓	✓
Energy pay back time (EPBT)	✓		
Acidification potential (AP)	✓	✓	✓

The **global warming potential** is calculated using the CO_2eq measurement unit, which corresponds to the equivalent amount of CO_2 emissions relative the sum of the impact of all greenhouse gas emissions (e.g. CH_4, SF_6, N_2O, HFC and PFC) on a 100-year time scale. The global warming potential is calculated differently for the embodied, operational and disposal carbon. For the embodied carbon emissions, the specific material quantity (SMQ) is multiplied by the effective carbon coefficient (ECC):

$$\mathrm{GWP}_{\mathrm{embodied}} = \mathrm{SMQ} \cdot \mathrm{ECC} \tag{2.1}$$

The measurement unit used for the ECC is $\mathrm{kg}_{\mathrm{CO2eq}}/\mathrm{kg}_{\mathrm{material}}$, according to the calculation method by Dias and Pooliyadda[81]. This leads to a measurement unit of $\mathrm{kg}_{\mathrm{material}}/\mathrm{m}^2$ for the SMQ, where m^2 is the functional unit, discussed later in Table 2.3. In literature, material weight per square meter is also referred to as 'material efficiency'[82]. Currently, material efficiency does not regularly drive design considerations, hence many buildings are not optimized for material used and embodied carbon emitted, which makes it a very relevant topic of research. A few researchers have tried to map material efficiency numbers for high-rise/skyscraper buildings[83], mentioning the definition "premium for height", as seen in Figure 2.2, and office buildings[32], as these are large scale projects, where a small percentage in material savings has a significant impact on total construction costs.

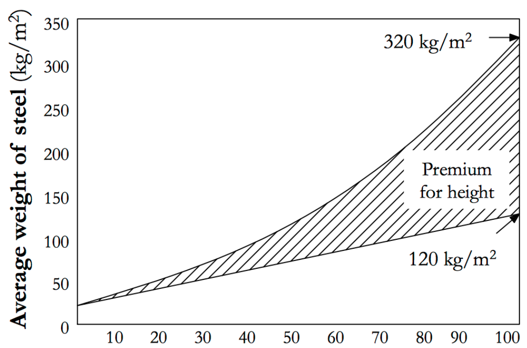

Figure 2.2: Material efficiency in relation to number of stories; a case study of 3482 tall buildings[3]

The ECC includes all emissions from raw material extraction, building material production, transport and construction. Hammond describes that there is gaps in data of embodied carbon coefficients and a general wide variability in datapoints[7]. The University of Bath has one of the most extensive database on embodied carbon and embodied energy coefficients, the inventory on carbon & emissions (ICE). Figure 2.3 gives an overview of the variability of embodied energy coefficients of cement over time from this database. As can be seen datapoints vary heavily for all time points. The same picture is seen for embodied carbon coefficients.

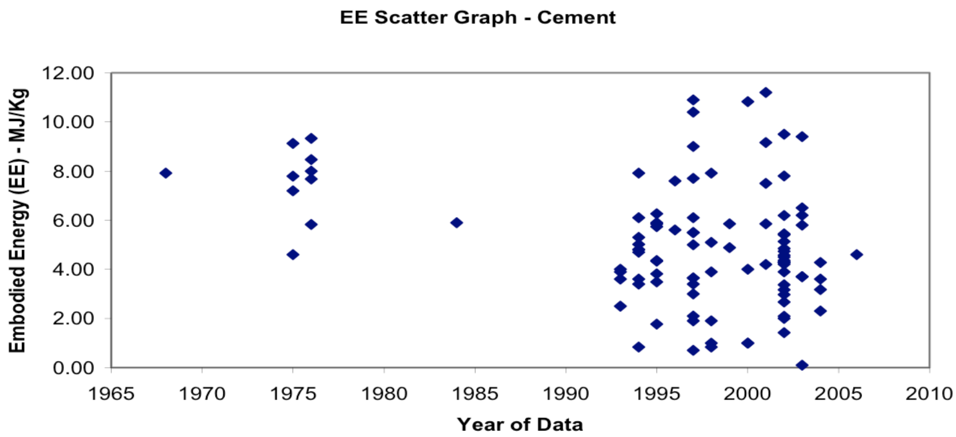

Figure 2.3: Variability in embodied energy data of cement over time[7]

For operational carbon emissions, the operational energy (OE) in MJ/m^2 is multiplied by the emission factor (EF) in kg_{CO2eq}/MJ:

$$\mathrm{GWP}_{\mathrm{operational}} = \mathrm{OE} \cdot \mathrm{EF} \tag{2.2}$$

For the disposal carbon, the processes of demolition and landfill contribute to the emissions for the global warming potential using the same segregation methodology between material quantity (SMQ) $kg_{material}/m^2$ and disposal carbon coefficient (DCC) $kg_{CO2eq}/kg_{material}$ as for the embodied carbon calculation.

$$\mathrm{GWP}_{\mathrm{disposal}} = \mathrm{SMQ} \cdot \mathrm{DCC} \tag{2.3}$$

The **gross energy requirement** uses the same methodology as GWP, as there is a significant amount of overlap. The difference is that the measurement unit MJ/m^2 is used instead of kg_{CO2eq}/m^2 for embodied, operational and disposal energy. Here embodied energy coefficients in $MJ/kg_{material}$ are used for the embodied energy calculation, according to Alcorn[84]:

$$\mathrm{GER}_{\mathrm{embodied}} = \mathrm{SMQ} \cdot \mathrm{EEC} \tag{2.4}$$

Operational energy in MJ/m^2 is directly calculated from the processes that require energy (heating, cooling etc.), as used in the operational carbon equation.

$$GER_{\text{operational}} = OE \tag{2.5}$$

The disposal energy is again based on the SMQ kg_{material}/m^2 and disposal energy coefficient (DEC) MJ/kg_{material}:

$$GER_{\text{disposal}} = SMQ \cdot DEC \tag{2.6}$$

The **energy pay back time**, relates mostly to the life cycle assessment of photovoltaic panels and is only used for the adaptive solar facade in this thesis. The methodology used is according to Raugei et al.[8], who compared the life cycle assessment of CdTe, CIS and poly-Si photovoltaic panels. They define the EPBT as: "the ratio of the GER to the avoided primary energy requirement for the production of the same amount of electricity delivered by the system (assuming the average conversion efficiency of the chosen electric mix)". The measurement unit for the EPBT is years. Figure 2.4 shows an example of the difference in EPBT of different photovoltaic technologies. The range lies within 1.5 and 5.5 years between poly silicon and CdTe panels respectively.

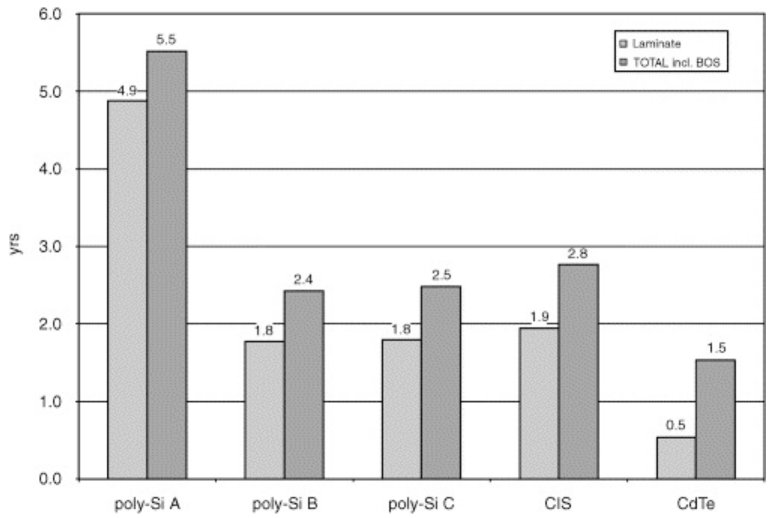

Figure 2.4: Variability energy pay back time of solar panels[8]

The **acidification potential** has the measurement unit SO_2eq/m^2 in kilogram. Again, the equivalent stands for emissions, such as SO_2, NO_x and NH_3. Adalberth et al.[60] and Peuportier[72] concluded that the acidification impact is highest when the main construction material consists out of concrete, hence this is an important impact factor for the thin-shell roof and funicular floor. Also, it is often used for the review of photovoltaic technologies[8], hence acidification potential is relevant for all technologies evaluated in this thesis. The acidification potential is calculated according to the same method as the gross energy requirement. The embodied acidification potential is calculated using SMW and embodied acidification coefficient (EAC). The operational acidification potential is the sum of SO_2/m^2 emissions, due to processes during the lifetime of the system. Finally the disposal acidification potential is calculated using the SMQ and disposal acidification coefficient (DAC).

$$\mathrm{AP}_{\mathrm{embodied}} = \mathrm{SMQ} \cdot \mathrm{EAC} \tag{2.7}$$

$$\mathrm{AP}_{\mathrm{operational}} = \mathrm{OA} \tag{2.8}$$

$$\mathrm{AP}_{\mathrm{disposal}} = \mathrm{SMQ} \cdot \mathrm{DAC} \tag{2.9}$$

The acidification potential is mostly SO_2 and NO_x emissions following from the transport of goods, therefore the higher the density of the material, the higher the acidification potential in general. Also, looking at a case study LCA on concrete, the raw material production process of concrete emits a significant amount of SO_2eq, which can be seen in Figure 2.5.

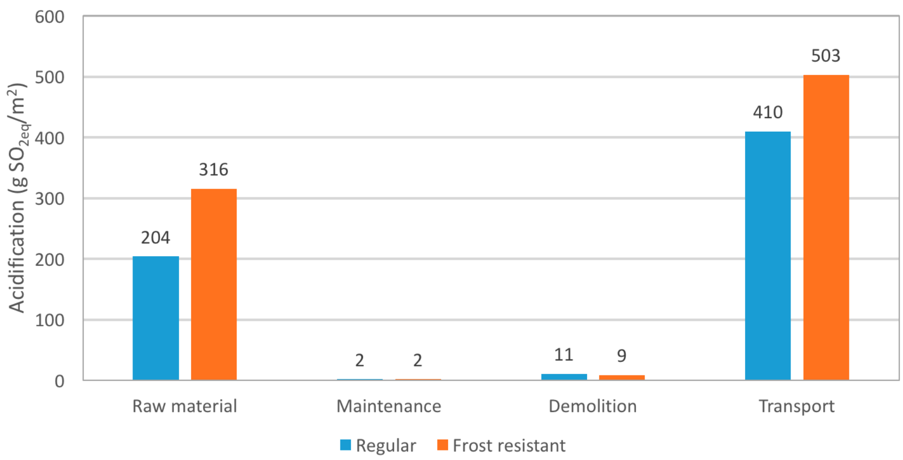

Figure 2.5: Concrete acidification break-up in grams of equivalent SO_2/m^2[9]

The **functional unit** for all three technologies is area in m^2. For the adaptive solar facade, floor surface area in the room behind the glass facade is used, while parallel floor surface area is used for the thin-shell roof and funicular floor. The functional unit makes the calculation independent on size, making an apples-to-apples comparison possible. The functional unit needs to describe the "primary functions fulfilled by the technology" according to the Handbook on Life Cycle Assessment[36]. Also, SI-unit denomination is preferred and advised. The functional unit can also be found in the material efficiency described earlier in this Chapter and many reference flows within the LCA or databases are measured relative to the functional unit. As the adaptive solar facade is both a shading system and a photovoltaic system, a second functional unit is used in kWh. In this way the ASF can be compared with shading systems using kg_{CO2eq}/m^2, while kg_{CO2eq}/kWh is used for the comparison with other photovoltaic systems.

Table 2.3: Overview of functional units per building technology

	ASF	Thin-shell roof	Funicular floor
Functional unit	m^2 | kWh	m^2	m^2

The kg_{CO2eq}/kWh metric is calculated by taking the total GWP of the system from the LCA and dividing this by the kWh produced over the lifetime of the solar panel. According to the guidelines of the International Energy Agency (IEA), the calculation of kWh produced needs to be based on conversion efficiency η, performance ratio PR, irradiation I, lifetime LT and area of the module A[85].

$$\frac{\mathrm{GWP}}{\mathrm{I} \cdot \eta \cdot \mathrm{PR} \cdot \mathrm{LT} \cdot \mathrm{A}} \tag{2.10}$$

Furthermore, the sources of information need to be specified by manufacturer, data collector and age of data. This fits the framework to ensure consistent and transparent lifecycle analyses for photovoltaic systems[86]:

- Completeness of reporting results and methods: use of functional units, scoping, inventory analysis and impact analysis
- Validity of analysis methods: calculation of grams dioxide equivalent per kilowatt-hour according to equation 2.10
- Relevance to present-day technologies: modern reference technologies

2.2.2 System boundaries

The system boundaries of the life cycle assessment determine which processes and material inputs are taken into account in the calculation. The system boundaries can be divided into horizontal and vertical boundaries. An example of a vertical system boundary is a product that goes from material extraction to demolition, also known as 'cradle to grave'. Other vertical boundaries are cradle to cradle (from material extraction to material reuse) or cradle to gate (from material extraction up to and including construction). The vertical system boundaries used in this thesis are generally according to 'cradle to grave', in line with Moncaster and Symons[87]. They describe a cradle to grave system boundary which is compliant with the European TC350 standard. This thesis uses three sub-processes for the cradle to grave process:

1. Embodied carbon, energy and acidification potential
2. Operational carbon, energy and acidification potential
3. Disposal carbon, energy and acidification potential[1]

Figure 2.6 shows a general process for a building system from cradle to grave. The process starts with raw material extraction, from this building products are made, which are then transported to the building site, where the construction takes place (embodied). After construction, the building system is used (operation) and then demolished and transported to either a landfill or recycling site (disposal).

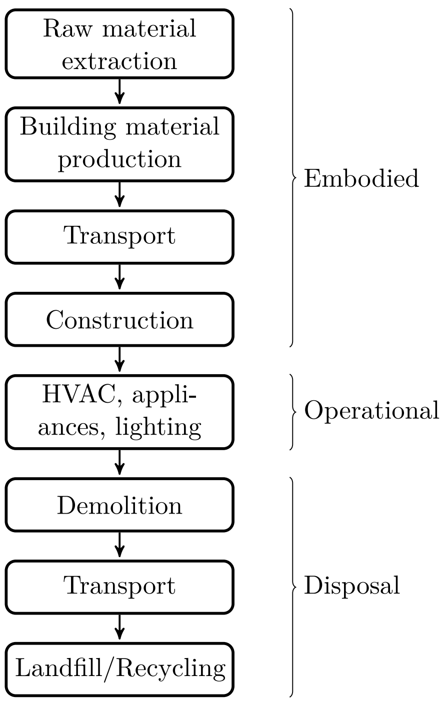

Figure 2.6: General cradle to grave process flow division

The **supporting structures** are also part of the scope/included in the system boundaries. The reason for this is that technologies within the building envelope are evaluated instead of a complete building project. Therefore a change in technology in the building envelope also changes the design of

[1] Can be neglected according to literature

the supporting structures. This is needed to create a fair comparison to the existing technologies. The system boundaries are, in this way, not only defined vertically in the chain, but also horizontally including the difference in supporting structures. The horizontal boundaries only include the supporting structural components for the technologies in the building envelope.

For photovoltaic systems, the term balance of systems (BOS) is used to refer to the supporting structures. This includes all structural supporting structures, but also electrical equipment such as inverters, voltage regulators and bypass diodes. The reason BOS is used, is because in this way both the performance of the solar panel itself and the supporting structure (in this thesis the adaptive solar facade structure) can be independently assessed. For the adaptive solar facade the focus lies more heavily on the BOS, therefore this approach enables a detailed and structured analysis of both the thin-film CIGS and BOS. The term BOS is also widely used in literature, hence this makes the method consistent with other assessments in literature.

The **cut-off approach** is used for recycling and landfill. This means that recycling does not generate any credit for the product and resulting benefits are not taken into account. Furthermore the use of recycled products do not bear the burden of processes higher up the chain. An example of this is recycled paper, here recycled paper does not carry the burden for the processing required to produce the primary paper. Furthermore primary paper does not get the benefits of creating new energy from waste incineration or new paper from recycling, it only carries the burden of the waste process. Many databases use this cut-off system model, which simplifies the life cycle assessment considerably. The main focus of this thesis lies on operational and embodied factors and their relationship, the emphasis does not lie on recycling, therefore the cut-off approach is chosen. The cut-off approach defines three types of end-products of a process[36][10]:

- Ordinary by-products: materials with economic value, which are not the reference product, but are created as result of producing the reference product
- Recyclable materials: materials with little economic value, which can serve as input or resource for recycling activity
- Waste products: materials with no economic value and no recycling potential

The bottom line of this approach is that disposal of products comes with burdens, however the resulting product (by-product or recycled material) is burden-free available for the next product. Therefore the LCA does not have to create scenario's of different types of benefits of reuse, but just simply accounts for the burdens of disposal/recycling. Thus, simplifying the life cycle assessment, while keeping relevance and a structured framework of allocation. The cut-off approach is also consistent with the "cradle to grave" system boundaries, where only costs of recycling or landfill are included, not the benefits. Figure 2.7 shows the cut-off points for all three products.

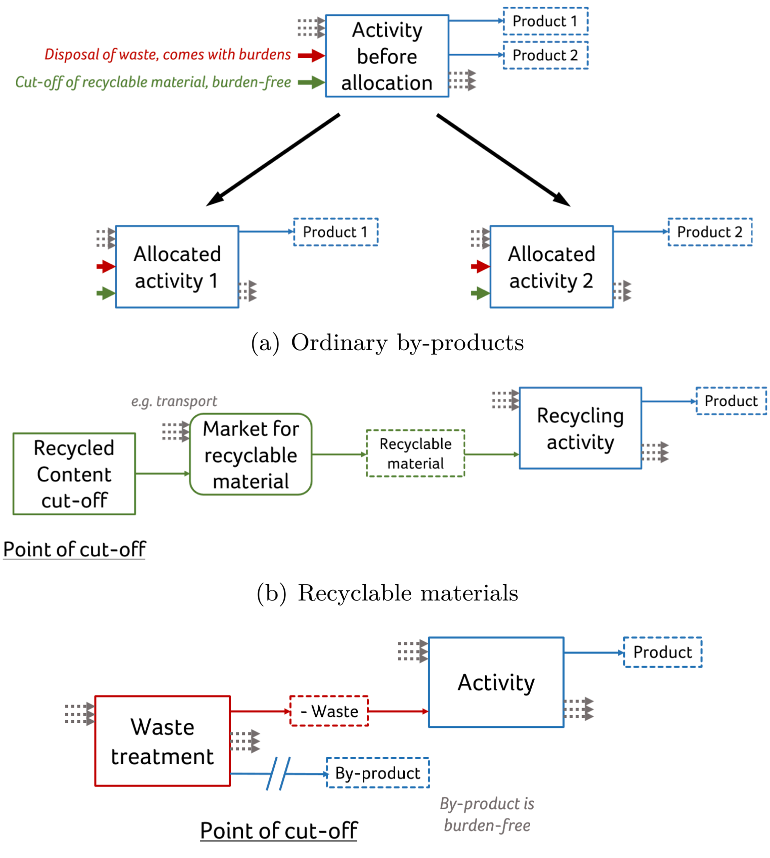

(a) Ordinary by-products

(b) Recyclable materials

(c) Waste products

Figure 2.7: Cut-off approach for three types of products[10]

2.3 Inventory analysis data

Looking at the LCA calculation methodology described previously, two types of data are needed for the inventory analysis: material quantities and impact category coefficients of materials and processes. The material quantities will be provided by technical drawings and personal conversations about the three technologies. The impact category coefficients will be provided by a life cycle inventory (LCI) database. This data, then leads to the final LCA with the use of an impact assessment tool. This section will first give an overview of LCI databases. Next, the chosen ecoinvent database for the impact category coefficients will be explained in detail, whereafter challenges of gathering LCI data and consistency issues concerning data definitions are addressed. Last, obtaining the material quantities through personal conversations and technical drawings is discussed.

2.3.1 Overview of existing LCI databases

In general, there are two types of LCI databases, both with different purposes:

- Material quantities and coefficients of existing building projects and case study databases
- Impact category coefficients databases of materials and processes

Databases with material quantities/coefficients generally hold a few hundred projects and are mostly in-house databases of engineering companies, examples are the Arup PECD and Thornton Tomasetti databases. These are in-house databases on their projects giving insight in structural material quantities used and corresponding embodied carbon emissions and embodied energy requirement[88]. A problem with these databases is the wide bandwidth of data points due to project specific applications and data gaps.

Impact category coefficient databases are mostly commercially available databases, such as GaBi and ecoinvent. These hold thousands of coefficients of materials, products and processes. These databases are most extensive and give the most consistent data, however are not transparent in compiling data, as they are not open-source.

Table 2.4 gives an overview of all existing databases and reports. As can be seen the major problem is discrepancy in data provided, where every database provides different data. Also definitions are generally not consistent leading to data gaps and inconsistencies and lack of transparency.

Because of the issues with consistency, this thesis chooses to use one database only, the ecoinvent LCI database. This database is most exhaustive and uses the most consistent approach on data collection, including the use of the cut-off approach as discussed earlier. Although the ecoinvent database is most exhaustive, data gaps are filled with assumptions, literature and data based on personal conversations. Every assumption will be mentioned in Chapter 3.

Table 2.4: Existing reports and databases[3]

Reports	**GWP**	**GER**	**AP**	**Reference**
Inventory of Carbon and Energy	✓	✓		[7]
Structure and Carbon	✓			[43]
Cole and Kernan	✓			[42]
Eaton and Amato	✓			[32]
Databases				
ARUP PECD	✓	✓		[88]
Ecoinvent	✓	✓	✓	[89]
GaBi	✓	✓	✓	[90]
Thornton Tomasetti	✓			[91]
U.S. LCI	✓	✓	✓	[92]

2.3.2 Ecoinvent LCI database

The Ecoinvent 3.1 LCI database is an impact category coefficients database for materials and processes. It is developed by ETH Zurich and holds over 11,000 LCI datasets. Different data is also available depending on geography, as for instance the electricity mix differs per country. This enables geographical impact analyses and can drive sourcing decisions. It is one of the largest databases available. One of the downsides of using this database is that it also holds older information. Working with rapidly changing processes, such as photovoltaic solar module production can therefore lead to problems, as the right processes need to be selected and existing processes can be outdated.

2.3.3 Challenges obtaining data

There are mainly four challenges regarding obtaining data for the LCA for an accurate, reliable and consistent assessment method: coefficient variability due to product assumptions, accurate quantities, coefficient range depending on database used and mutually exclusive collectively exhaustive (MECE) allocation of processes. Most of these challenges occur due to either a lack of data on a process or different use of assumptions and can significantly change the final result on the LCA. It is very important to try to split these factors in a driver tree, as shown in Figure 2.8, to analyze each factor and do a sensitivity analysis on each driver, which is done in Chapter 3. The red box shows the mathematical drivers, coefficient and quantity, while the blue box shows the organizational drivers, database used and allocation of processes.

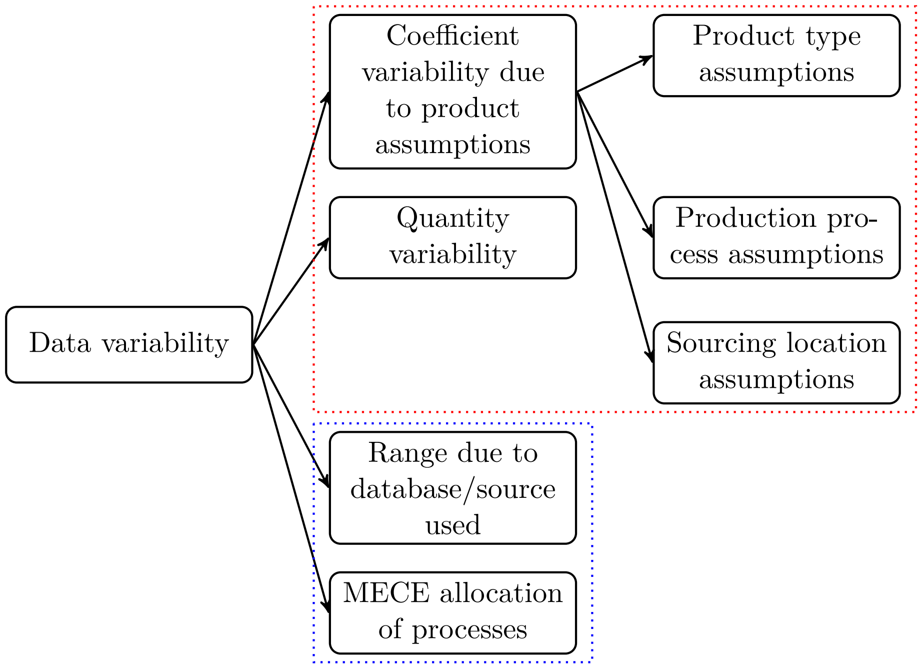

Figure 2.8: Driver tree of data variability

Coefficient variability due to product assumptions

Coefficient variability due to product assumptions can be broken down into three aspects: product type, production process and sourcing location assumptions.

First, the **product type** chosen (e.g. form factor or strength of the material) determines the coefficient significantly, as processes differ based on product type manufactured from the same material. Another example of this is high voltage electricity versus low voltage electricity.

Second, **process assumptions** (e.g. recycling ratio or average transport distance) also influences the coefficient. The end product is exactly the same, the process to create the end product is the same, however different assumptions are made on the ratio of quantities used during the process to get to the final ECC for the product.

Figure 2.9 shows the different coefficients for steel related to form factor (product type) and recycling (process assumptions). It can be seen has recycling is linear relationship to the ECC of steel. Also, galvanized sheet steel is roughly 10 percent worse than non-galvanized sheet steel. Next to this there are more product type and production process assumptions for steel, such as alloy type and hardened versus unhardened steel.

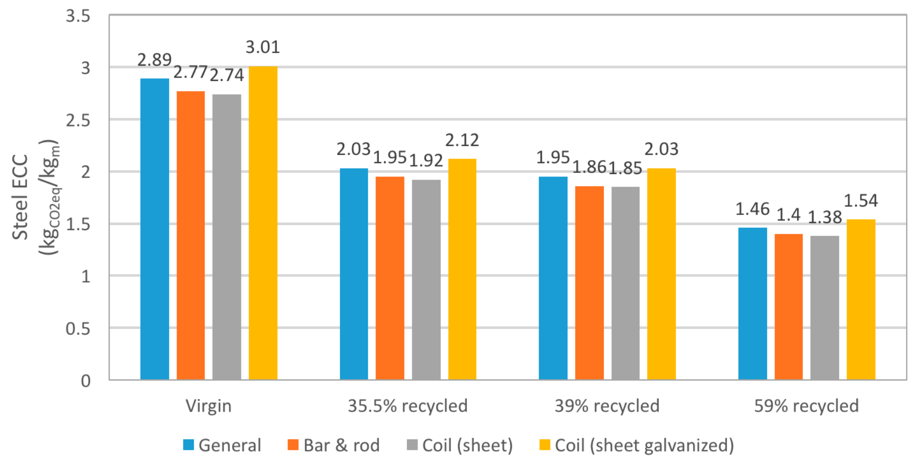

Figure 2.9: Variability in ECC for steel due to product type (product form) and process assumptions (recycling ratio)[7]

Third, **sourcing location** can greatly influence the coefficients. For solar cell production, electricity is the main contributor to the final GWP. However the electricity mix in Switzerland has a lower ECC than the electricity mix in Germany or the United States of America. Therefore the sourcing location creates a variability for the same end product. Figure 2.10 shows different electricity mix values, the GWP per kwh in China is $1145.8g_{CO2eq}/kWh$, while in Switzerland this is only $119.6g_{CO2eq}/kWh$. The large difference of a factor 9-10, therefore means that the sourcing location used is of main importance for a GWP LCA on solar panels, instead of the technology used.

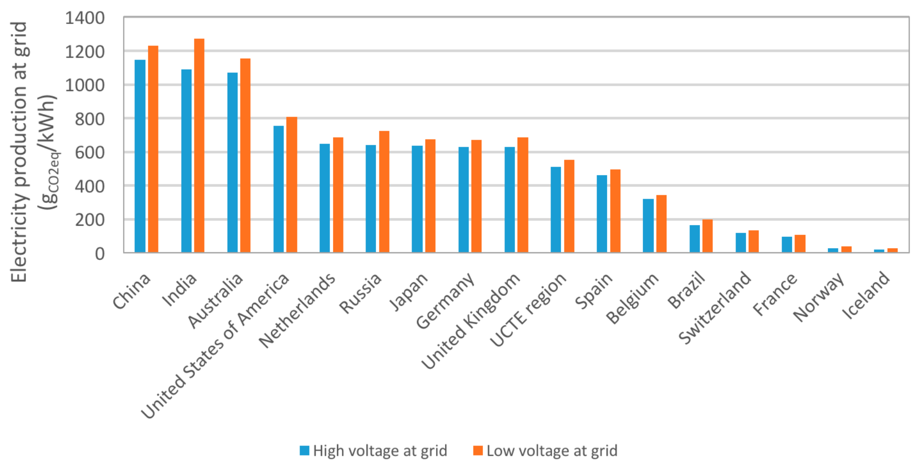

Figure 2.10: Variability in ECC of sourcing location of electricity production [11]

Accurate quantities

As this thesis evaluates new unconventional building technologies, personal conversions, technical drawings and supply material purchasing bills are most accurate determining quantities used of specific products. Also specific products have been weighted and measured, e.g. the weight of bolts, screws and nuts or the thickness and length of cable wire used. Getting accurate quantities however also applies to quantities of material used in different product processes from the database. This means that specific product processes are altered to simulate the exact production process of the product used.

Coefficient range depending on database/sources used

The choice of database can significantly influence the coefficient of a specific material or product. Figure 2.11 shows the coefficient difference between four different databases for the same process definition and location: Hot-rolled, low alloyed steel manufactured in the RER region. It can be seen that the Ecoinvent database shows a value which is more than twice as high as the ICA Bath database.

These differences, depending on the database, can have a variety of reasons. These vary from using different weighted average calculations to a different date of data collection or different measuring technique or location (by factory or company). In this way the apparent same process or product can be still give a different coefficient depending on the database used. For this reason only one database is used for all calculations in this thesis, This is the Ecoinvent v3.1 database, as described earlier.

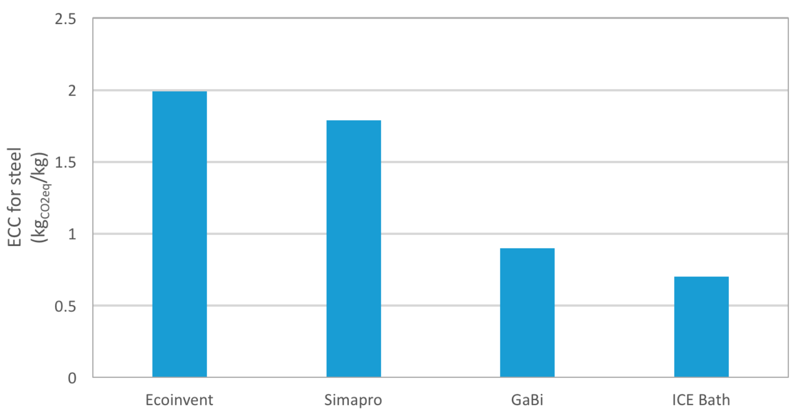

Figure 2.11: Hot-rolled, low alloyed, steel ECC from different sources manufactured in the RER region[3]

Mutually exclusive, collectively exhaustive allocation of processes

MECE allocation of processes means that there can be no overlap or gap between processes. This means, if a collection of processes is used to create a product, these processes need to be checked individually if there is overlap or a gap between these processes to create this product. This can be a very elaborate task because, as seen above, there are a variety of reasons why one process can be different than the other. Therefore it is not always clear where an overlap or gap in the production processes can be manifested.

2.3.4 Personal conversations and literature

Personal conversations with the designers of the technologies at ETH Zurich and literature are both used to verify and validate the data used. These technologies are still in the experimental phase, therefore verification and validation via personal conversations and bench-marking against other research leads to a comprehensive result of the case studies, as not all information is documented at this stage and the designs are solely case studies.

2.4 Impact assessment tools

Impact assessment tools are software applications that facilitate life cycle assessments. These tools typically structure the calculation, by creating an interface between the database and the input parameters that automatically calculates the impact characteristics of the process, product or case study of interest. The choice of the right assessment tool together with the indicator score conversion method can influence the assessment and is therefore discussed in this section.

Table 2.5: Selection of impact assessment tools with corresponding provider

Assessment tool	**Software provider**
SimaPro	PRe Sustainability
GaBi	thinkstep
Umberto	Ifu Hamburg
OpenLCA	GreenDelta
eBalance	IKE Environment Technology
EIME	Bureau Veritas CODDE
Quantis Suite	Quantis
Team 5	PWC
REGIS	sinum

2.4.1 Overview of existing LCA tools

Table 2.5 shows the main life cycle impact assessment tools available on the market. Most of them are license based (e.g. SimaPro, GaBi and Umberto), while others are open-source without any license fee (e.g. OpenLCA). The most frequently used tools are SimaPro, Gabi, Umberto and OpenLCA, where SimaPro is the oldest and most widely used tool on the market.

Articles published in the International Journal of Life Cycle Assessment and Journal of Industrial Ecology have been using mostly Simapro and GaBi from 2010-2013, however in recent years other life cycle tools started to be used more frequently, e.g. Umberto and OpenLCA[12]. Figure 2.12 shows the number of articles published per impact assessment tool. It is important to notice that in 2014 "other tools" have become more widely used.

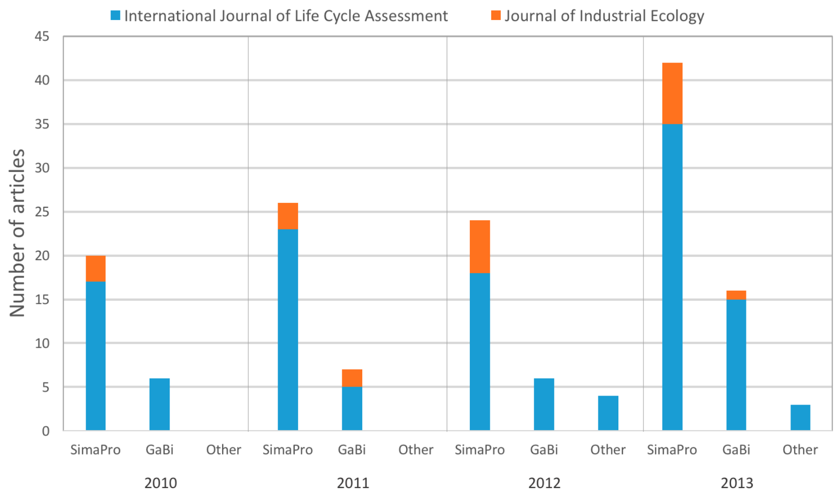

Figure 2.12: From 2010 to 2013 SimaPro has been the leading assessment tool, followed by GaBi[12]

The choice of tool is important, as a recent study showed that when identical assessments are done in both SimaPro and Gabi there is a difference in reported impacts of up to 20 percent[12]. The study attributed this change mainly to the use of slightly different characterization factors. Giving rise to the indication that there are slight variations in the many assumptions used by the tools.

Therefore it is important to use a tool where you either can verify and validate the assessment in detail or a tool that is (or will be) used in the majority of journal articles, therefore making simple comparison of results possible between studies. The choice of tool in this thesis is OpenLCA v1.4.2.

2.4.2 OpenLCA v1.4.2

OpenLCA is developed by GreenDelta as a free LCA platform. Below, five reasons are described, why this tool is chosen.

First, the tool is open-source, therefore a calculation can be checked in detail for review and functionality of the program is able to increase exponentially based on the amount of users.

Second, there are no license costs. Therefore simple peer-reviewed sharing is possible, as anybody can download the tool and go through every detail of the calculation.

Third, OpenLCA has an increasingly growing user base. Therefore the assumption made for this thesis is that this software will become mainstream in the research community therefore making it possible to compare results from OpenLCA with assessments of others using the same impact assessment tool.

Fourth, the tool works for both Windows and OS X making sharing across platforms easy. This also simplified peer-reviewing, as there is no limit based on computer operating system.

Last, all LCA functions needed for this thesis are present. There is no reason to use a more elaborate tool, like SimaPro, which has more limited peer-review and calculation review options, as it is not open-source, carries a license fee and only works on a windows operating system.

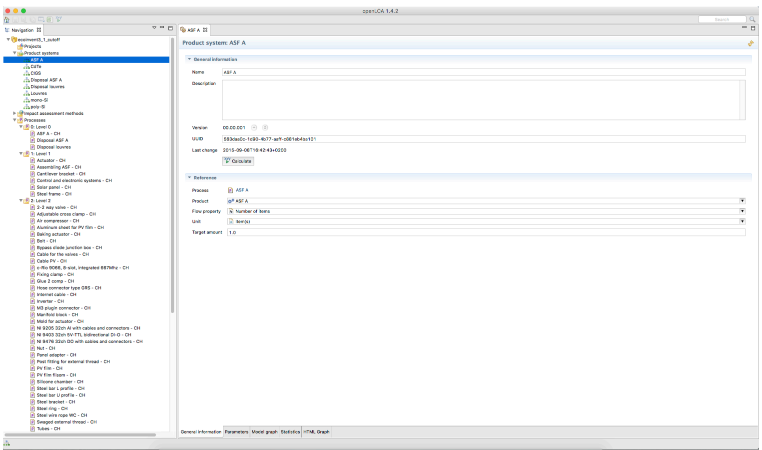

Figure 2.13: Screenshot of the OpenLCA v1.4.2 interface

2.4.3 Indicator score conversion method

The indicator score conversion method used is Recipe Midpoint-H. The ISO guidelines only provide a generic framework, therefore the choice of indicator score conversion method determines how the LCI result creates the LCA result. The recipe method was developed to combine the "problem oriented approach" of CML-IA with the "damage oriented approach" of Eco-indicator 99. For this thesis only the problem oriented approach is used (Recipe-midpoint).

Looking at Figure 2.14, midpoint impacts are parameters such as water use, energy content, global warming potential and PM10 concentration. These midpoint parameters can be established with relatively low uncertainty as it mostly comprises out of quantities of harmful materials (e.g. methane, water use, particulate matter etc.). The damages caused by these quantities of harmful materials are the endpoint of the recipe method. The endpoint parameters have a relative high uncertainty, as it is mostly very hard to predict what the damage of certain materials will be over a very long time period. The endpoints are divided into damage to human health (disability-adjusted life year), damage to ecosystems (species year) and damage to resource availability (resources surplus cost).

The incompleteness and uncertainty following from the midpoint parameters are based on the state of art knowledge currently available. Therefore three scenario's with assumptions were developed. This thesis uses the hierachist (H) perspective. The hierachist perspective uses the most widely used policy assumptions. Nest to the hierachist perspective, the individualist (I) and egalitarian (E) perspectives exist for the midpoint parameters, however are not used for this thesis.

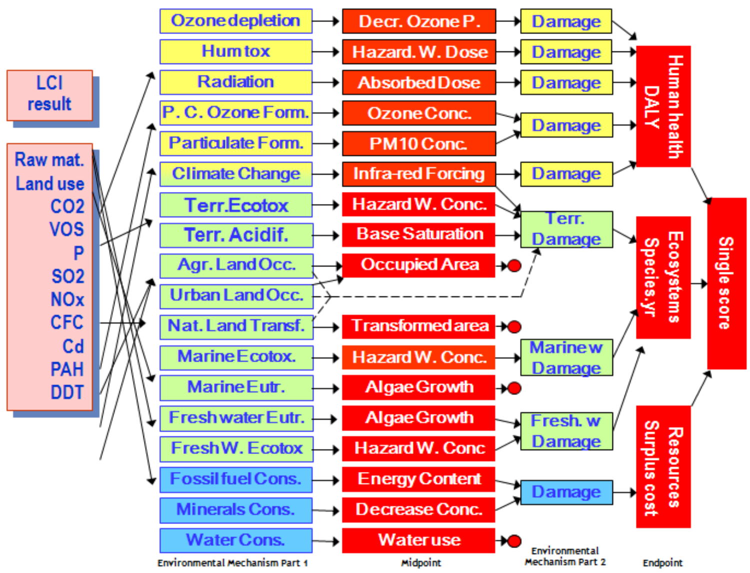

Figure 2.14: Connection between midpoint (low uncertainty) and endpoint (high uncertainty) impacts[13]

Chapter 3

Survey of technologies in HiLo building

This chapter shows the results from the LCA for the three case studies of the Hilo building. The three technologies are compared to other existing technologies. Also a Monte carlo simulation and sensitivity analysis is done on the LCA result to account for uncertainties in the calculation and data. Last design considerations are given to optimize the design of the technologies.

3.1 Case study I: Adaptive Solar Facade

The case study for the adaptive solar facade is based on 'facade A' developed for the Hilo building unit to be constructed for the NEST project in partnership with EMPA and EAWAG in Dubendorf, Switzerland. The facade has an area of 8.96m^2 and holds an array of 36 adaptive solar panels. Figure 3.1 shows one of these adaptive panels, which includes the solar panel, actuator, cantilever brackets and fixing clamps to the steel frame.

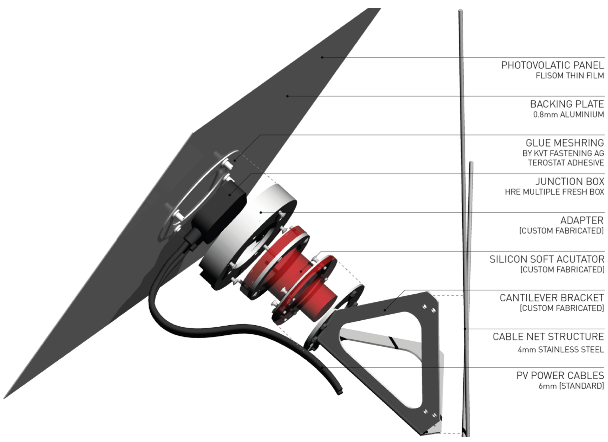

Figure 3.1: Single adaptive solar module attached to the steel frame[14]

3.1.1 Overview

Technical description

The ASF has three functions: shading of direct sunlight, allowance of diffuse sunlight and solar tracking for the photovoltaic panels. These functions reduce the cooling, heating and lighting needed for the room and increases the electricity production of the solar panels respectively. The algorithm, which controls the panels, finds the optimum position of each panel, this depends on the solar irradiation in kWh/m^2, room temperature in degrees Celsius and occupant preferred lighting intensity in lux.

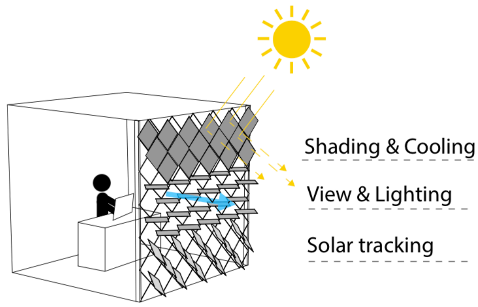

Figure 3.2: Three functions of the ASF[14]

The facade is a compiled product system (level 0) consisting out of six sub-product systems (level 1). Each of these sub-product systems is created using products (level 2), which are created using ecoinvent database processes. Therefore level zero, one and two are used to structure the ecoinvent processes into product systems and products respectively. Figure 3.3 shows the breakdown of the adaptive solar facade from level 0 to level 1.

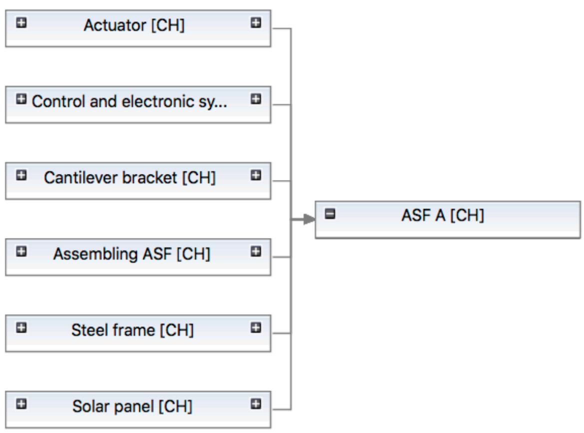

Figure 3.3: Breakdown of the adaptive solar facade into 6 sub-product systems

During the production of the adaptive solar facade product system, sub-product systems are used more than once, therefore ASF consists out of: 36 actuators, 1 control and electronics system, 36 cantilever brackets, 1 assembling ASF, 1 steel frame and 36 solar panels.

Table 3.1 shows all products included in the sub-product systems. Products can be used more than once for each sub-product system, however this can be found in Appendix C. Also, a detailed explanation of the creation of products out of ecoinvent processes can be found in Appendix C.

Table 3.1: Overview of products included in the six sub-product systems

	Actuator	Control and elec. system	Cantilever bracket	Steel frame	Solar panel	Assembling ASF
Glue 2 component	✓					
Tube 3mm PUN-H-3X0.5-NT	✓					
Silicone chamber elastosil	✓					
Panel adapter	✓					
Steel ring	✓					
Hose connector type GRS 4-3	✓					
Mold for actuator	✓					
Bolt 4mm	✓		✓	✓		
Nut 4mm	✓			✓		
Washer 4mm	✓			✓		
Vacuuming actuator 1 min	✓					
Baking actuator 60 min at 70C	✓					
NI9476 32ch DO with cables & connectors		✓				
NI9403 32ch 5V-TTL bi-directional DI/O		✓				
NI9205 32ch AI with cables & connectors		✓				
c-Rio 9066, 8-slot, integrated 667Mhz		✓				
Internet cable CAT-5E Ethernet		✓				
Inverter 1.25kW		✓				
Bypass diode junction box		✓				
2/2 solenoid valve MHA1-M1H-2/2G-0.9-HC		✓				
Cable PV		✓				
M3 plugin connector QSM-M3-3-1		✓				
Voltage regulator		✓				
Air compressor 0.75kW		✓				
Manifold block MHA1-P10-M3		✓				
Cable for the valve: KMH-0.5		✓				
Fixing clamp			✓			
Steel bracket			✓			
Steel bar U profile				✓		
Steel bar L profile				✓		
Adjustable cross clamp 4mm JAKOB				✓		
Swaged external thread swivel end 4mm JAKOB				✓		
Post fitting for exertal thread 4mm JAKOB				✓		
Stainless steel wire rope 4mm JAKOB				✓		
Aluminum plate 40x40cm (AlMg1 EN 573-3), anodized					✓	
CIGS PV film 40x40cm					✓	
Glue 2 component					✓	
Hydrolic hoist 3.5t MX20, idle for 8 hours						✓

Flow diagram

The flow diagram of the ASF, Figure 3.4, shows the major processes of the ASF during the lifetime of the product, divided into CIGS thin-film (green) and the ASF BOS (blue). First, for the CIGS thin-film, raw material is extracted using processes such as: mining of metals and other minerals, extracting of oil and lumbering wood. Second, base products are produced using processes such as: polymerization, forming, mixing, purification, cutting, alloying and heat treatment. Third the CIGS semiconductor is deposited on flexible polyimide foil using co-evaporation, according to Figure 3.5. Fourth, the PV module is created by submodule sorting and cutting, laminating the roll. Next the BOS product systems are added and the ASF is installed. Operation is simulated based on location, ASF and solar cell parameters, after this maintenance costs over the lifetime of the simulation are added. Last, the ASF is disposed.

The white boxes represent processes, which can be inputted into OpenLCA for the assessment. Grey boxes represent parameter assumptions and the orange box represents the simulation for operation. These boxes will be referred to later in the results section, when e.g. location, ASF and solar cell parameters are discussed in detail or when the simulation results are discussed.

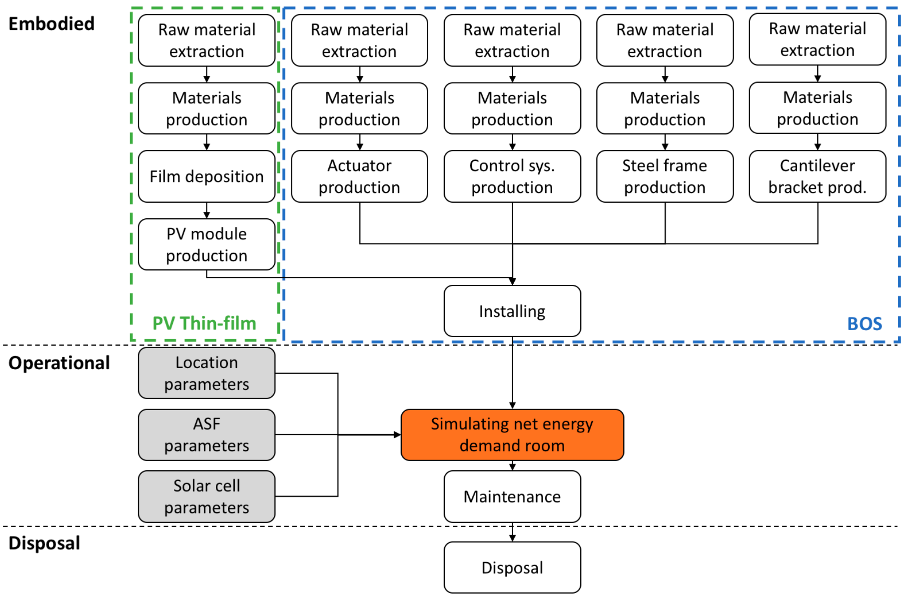

Figure 3.4: White boxes show the processes input into OpenLCA; grey boxes refers to the operation parameters for the simulation; orange box gives the simulation for operation results. The whole model is divided into an embodied, operational and disposal section

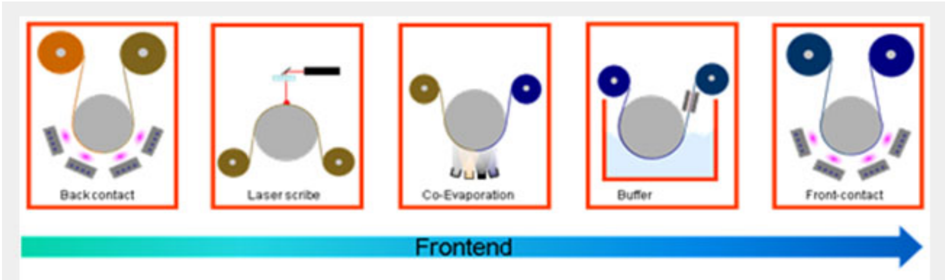

Figure 3.5: Five stage process of the deposition of CIGS (Cu(In,Ga)Se2) on polyimide flexible foil [15]

Inventory analysis

Before the life cycle impact assessment is done, it is important to analyze where certain quantities of materials are used in the design, this is called an inventory analysis. As an example, chromium steel 18/8 hot rolled is known for having a high carbon emission factor, therefore by analyzing the quantities used in the design, it is possible to pinpoint certain area's which can potentially be improved.

Figure 3.6 shows that chromium hot rolled steel is mainly used in the frame, 80 kilogram is used in the frame, while only 14.4 kilograms is used for the cantilever brackets and 10.8 kilograms for the rings that hold the actuator in place. Therefore improvements in the quantity of material used in the frame or different material use in the frame, e.g. use of low-alloyed steel, will lead to the greatest reductions.

Next to chromium steel, aluminum alloy also has a high carbon emission factor. Aluminum alloy is only present in the anodized sheet, where the PV film is attached to. 16.1 kilogram of aluminum alloy is used in the entire adaptive solar facade. Therefore making the aluminum sheet thinner will lead to reductions in embodied carbon, however 16.1 kilogram of aluminum used in the sheet for PV film is considerably lower than the 80 kilogram used for the frame of the ASF.

Also, in photovoltaic systems, the solar cells are commonly the main contributor to embodied carbon emissions. The ASF uses 5.8m^2 of CGIS thin-film. Last, control units and other electronics are usually a large contributor to embodied carbon. Figure 3.6 shows that the 2-2 way valves use the most electronics at 1.45 kilogram, followed by the voltage regulator and control modules.

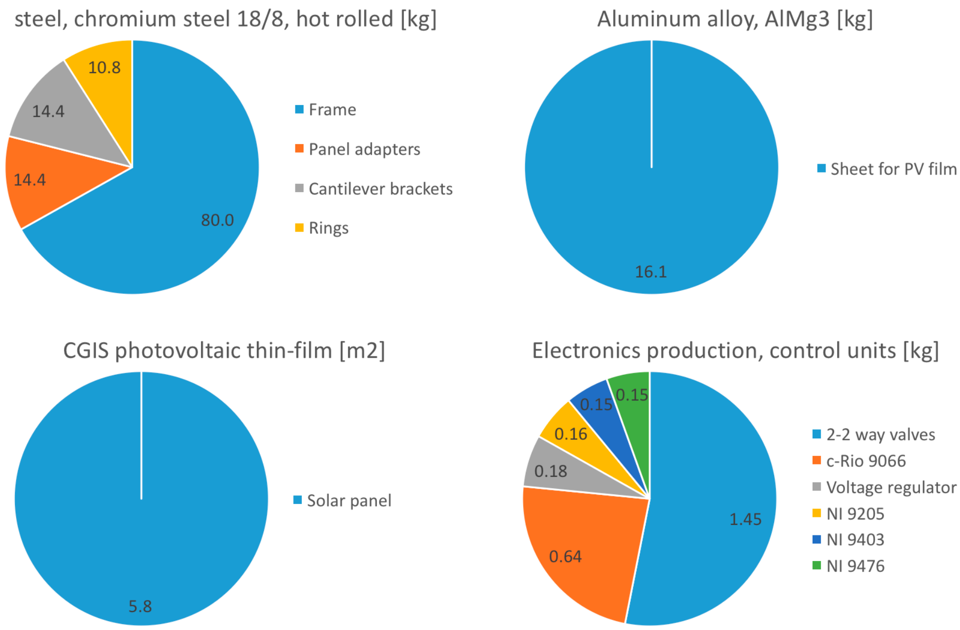

Figure 3.6: Distribution of four materials in the ASF design: chromium steel hot rolled, aluminum alloy AlMg3, CGIS thin-film and electronics production control units

3.1.2 Life cycle assessment

For the lifecycle asssessment several assumptions are used, as already discussed in the flow diagram in Figure 3.4. The solar cell assumptions (1-5), based on equation 2.10, and maintenance assumptions (6) are given by:

1. Solar irradiation Zurich, Switzerland: 1240 kWh/m^2/yr
2. Module efficiency CIGS: 14.5%
3. Performance ratio with optimal algorithm: 0.259[1]
4. Electricity production: 46.54 kWh/m^2; 417 kWh
5. Lifetime: 15 years
6. Maintenance every 5 years: 69.9 kg$_{CO_2 eq}$[2]

[1] Based on full facade area of 8.96m^2; Actual PV film area only comprises of 5.76m^2

[2] Includes: baking and vacuuming actuator, actuator silicone, actuator mold and idling hoist for 8 hours

The location and ASF assumptions are found in Table 3.2. The location assumptions are given by the weather location, office envelope, thermal set points, lighting control and occupancy assumptions. The ASF assumptions are given by solar reflectance and visible reflectance.

Table 3.2: Location and ASF parameter assumptions[14]

Office envelope	Roof: adiabatic Floor: adiabatic Walls: adiabatic Window: double glazed LoE ($\epsilon = 0.2$), 3mm/13mm air Floor area: 21.7 m^2
Thermal set points	Heating: 22 degrees Celsius Cooling: 26 degrees Celsius
Lighting control	Lighting set point: 11.8 W/m^2 Lighting control: 300 lux threshold
Occupancy	Office: weekdays from 8:00-18:00 People set point: 0.1 persons/m^2 Infiltration: 0.5 per hour
Adaptive solar facade	Solar reflectance: 0.5 Visible reflectance: 0.5
Weather file	Geneva, Switzerland (067000 IWEC)

The simulation gives the net energy demand as output, divided into a heating, lighting and cooling demand. Here three scenario's are calculated: no shading, louvres at 45 degrees fixed and the adaptive solar facade. This is done, so that savings relative to a base scenario and relative to an alternative technology (static louvres) can be determined.

Next, the net energy demand in GJ is converted into an electricity equivalent in kWh, as seen in Table 3.3. This conversion is done using the assumption that heating and cooling is done via a heat pump (COP of 3.9 and 2.8 respectively) and LED lighting is installed in the room. This electricity demand in kWh can then be used to calculate a carbondioxide equivalent in kg, using the emission coefficient of the Swiss low voltage grid (at the demand side). As shown in Table 3.3 both the louvres and adaptive solar facade show a reduction in both electricity demand and corresponding carbon emissions. It is important to note that for both the louvres as the ASF the heating and lighting demand increases, as less sunlight can enter the room. As the ASF is adaptive, this effect is smaller than with the use of louvres. This increase in energy demand is however offset by the cooling demand, which is greatly reduced with the ASF, leading to an overall reduction of 61.3 and 53.1 percent for the ASF and louvres respectively. It is important to note that Switzerland has a very low carbon emission factor for low voltage electricity from the grid. Therefore using a case study, where the room is located in Germany will give significantly different results and is discussed in the sensitivity analysis.

Table 3.3: Net yearly energy demand office room[14]

	No shading	**Louvres 45deg**	**ASF**
Heating (GJ)	2.92	3.33	2.96
Lighting (GJ)	0.98	1.04	1.01
Cooling (GJ)	8.51	2.85	1.50
Total (GJ)	**12.41**	**7.22**	**5.47**
Heating[a] (kWh)	208.0	237.2	210.8
Lighting[b] (kWh)	74.3	78.7	76.3
Cooling[c] (kWh)	844.3	282.7	148.6
Total (kWh)	**1126.6**	**598.6**	**435.7**
kg_{CO_2eq} (CH grid, low voltage)	**152.1**	**80.8**	**58.8**

[a]average COP of 3.9
[b]LED lighting
[c]average COP of 2.8

Global warming potential

From Figure 3.7 it can be seen that the biggest embodied GWP contribution in the ASF comes from the solar panels, control and electronics systems and steel frame. This is similar to the result from the inventory analysis, where the biggest amount of materials with known high carbon emission factors where present in these three product systems.

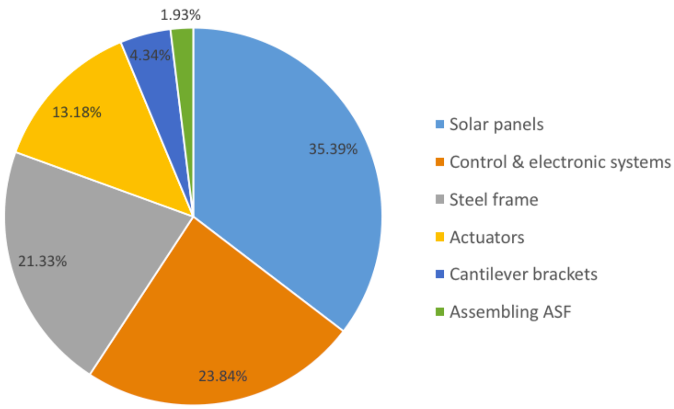

Figure 3.7: Embodied GWP contribution per segment of the ASF

Solar panels, control and electronics systems and chromium steel have an energy intensive production process. As the cut-off method is used the calculation does not benefit from recycling of steel. Benefits of recycling steel are only found in the sourcing of steel via the market mix, which with chromium steel is limited.

The global distribution of embodied GWP emissions is mostly focused on the European area, specifically Germany and Switzerland. This is in line of expectations as most production work for the ASF is done in Germany. It also can be seen however that emissions occur roughly everywhere in the world. This is mostly the sourcing of primary materials from a wide variety of locations around the world.

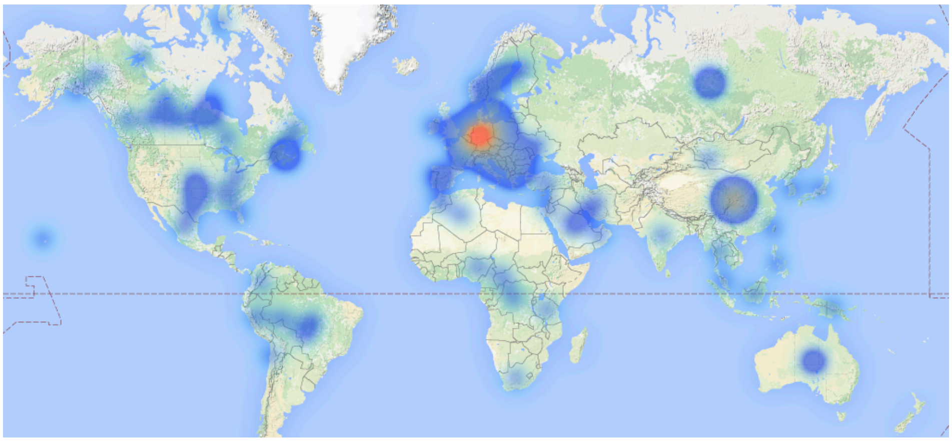

Figure 3.8: Global distribution of embodied GWP emissions from the production of the ASF

The total GWP of the ASF can be built up using a waterfall chart. Figure 3.9 shows subsequently the impact of embodied emissions, energy savings offset, maintenance and disposal. This leads to a total of 793.3 (kg_{CO_2eq}). When divided by the functional unit total electricity produced over the lifetime of the ASF, this gives a GWP of 126.8 grams of carbon doixide equivalent per kWh produced.

It can be seen that a significant initial investment of embodied carbon is needed to build the ASF and that most of this initial investment is offset by the heating, cooling and lighting demand reduction. Also maintenance of the ASF and disposal processes take up roughly 10 percent of all total carbon emissions. This total excludes the benefits of producing electricity, as this total is used to calculate the emission factor of electricity produced by the ASF (126.8gCO_2/kWh).

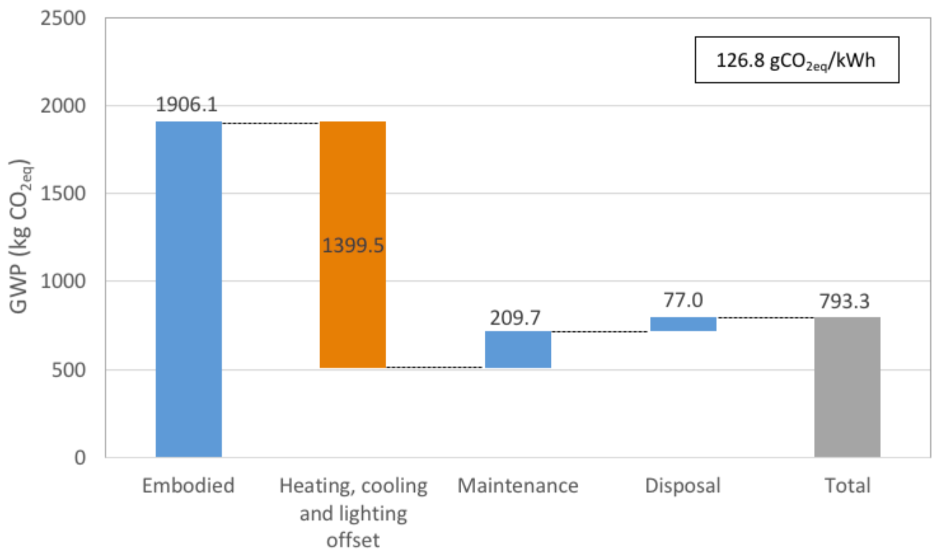

Figure 3.9: Build-up of total GWP of the ASF separated in components embodied, energy demand offset, maintenance and disposal

The amount of carbon emissions per kWh produced corresponds to a 6.1 percent reduction compared to the average electricity mix at low voltage in Switzerland. In Germany however the ASF has a 81.1 percent reduction in carbon emissions compared to the average electricity mix at low voltage. Figure 3.10 shows that the ASF performs better than the average electricity mix in terms of carbon emissions in mostly all countries, except France, Norway and Iceland.

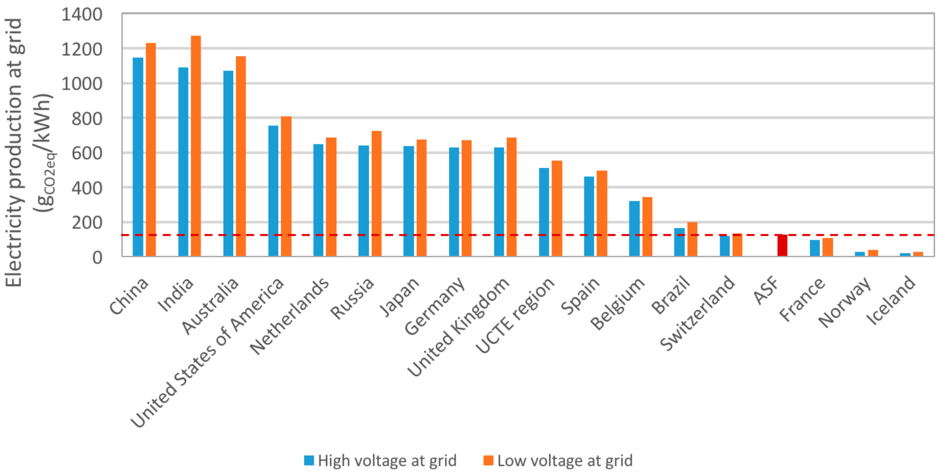

Figure 3.10: ASF (red) leads to reductions of carbon emissions per kWh compared to average electricity mix in most countries in the world

When including the PV production benefits based on the average electricity mix in Switzerland, an overall benefit of $51.1kg_{CO_2eq}$ can be achieved. This significantly increases when the ASF is placed in a country with higher emissions per kWh in their electricity mix (e.g. Germany, Spain or the United States of America). This then leads to a reduction of $2.4kgCO_2/m^2$ and $0.2\ kgCO_2/m^2 * yr$, when divided by floor area behind the facade.

Table 3.4: Difference of excluding and including benefits for PV production in total emissions

	ASF (ex. PV prod.)	**ASF (in. PV prod.)**
Embodied (kg_{CO_2eq})	1906.1	1906.1
HVAC (kg_{CO_2eq})	-1399.5	-1399.5
PV prod. (kg_{CO_2eq})	0.0	-844.4
Maintenance (kg_{CO_2eq})	209.7	209.7
Disposal (kg_{CO_2eq})	77.0	77.0
Total (kg_{CO_2eq})	**793.3**	**-51.1**
Total (gCO_2/kWh)	126.8	NA
Total ($kgCO_2/m^2$)	36.6	-2.4
Total ($kgCO_2/m^2 * yr$)	2.4	-0.2

Terrestrial acidification potential

As discussed in the method section, acidification potential of the ASF is also analyzed. Acidification has a local/regional impact, compared to carbon emissions. Therefore it is most interesting to look first at the spread of embodied emissions in $kgSO_2eq$ around the world. From Figure 3.11 it can be seen that China caries the highest burden of terrestrial acidification from production of the ASF.

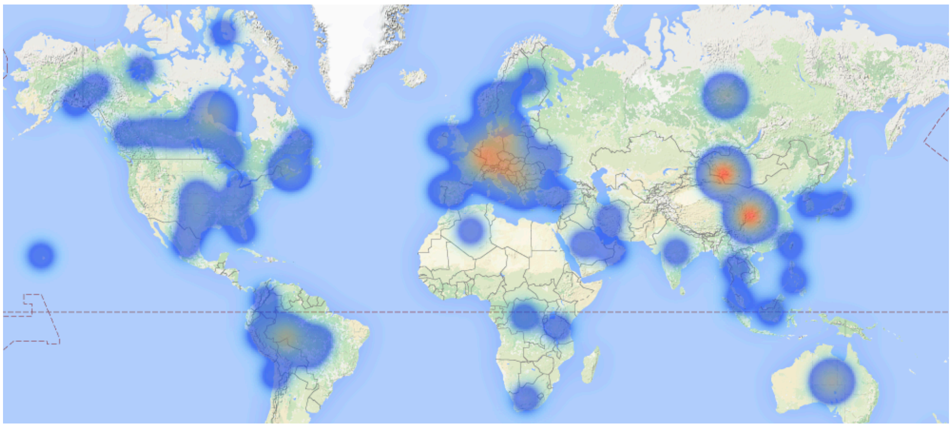

Figure 3.11: Embodied acidification impact spread out over the world

Also, Europe and North America show relatively high embodied emissions of SO_2eq. The fact that this impact is more spread out is greatly influenced by the fact that the total emissions are small, therefore a lot of very small contributions are spread out over the world contributing to the total amount. The total embodied emissions are 14.97 kgSO_2eq. The major contributor are the control and electronic systems, followed by the steel frame and solar panels.

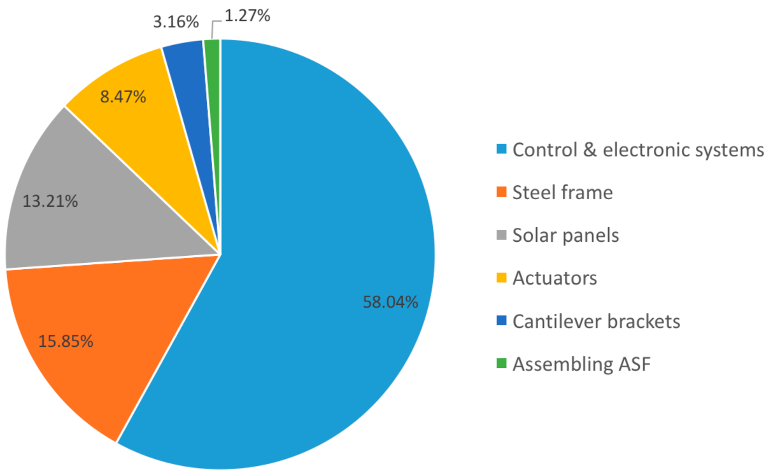

Figure 3.12: Embodied terrestrial acidification contribution per segment of the ASF

Total acidification potential emissions including maintenance and disposal contributes to 18.90 kgSO_2eq. Here, maintenance requires 3.80 kgSO_2eq and disposal 0.12 kgSO_2eq.

Energy pay back time

The energy pay back time refers to the time it takes for the operational energy reduction can pay back the embodied energy. The ASF has 23.36GJ of embodied energy (557.83743 kg oil equivalent). The yearly net energy demand and electricity production contributes to 3.40GJ. When yearly maintenance of 0.09GJ is subtracted the total yearly operational savings are 3.31GJ. Therefore the energy pay back time is 7.05 years. Figure 3.13 shows the cumulative energy requirement of the ASF, here also the disposal energy is visible at end of life (EOL). It can also be seen that the ASF roughly saves twice as much energy during its lifetime than it has cost to produce. The energy required for disposal is minimal and only 0.4 percent of the embodied energy required.

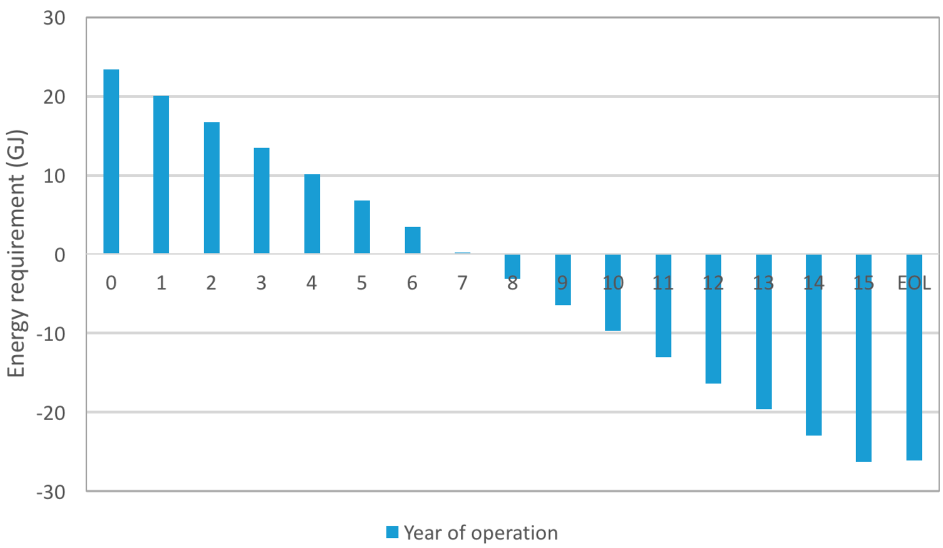

Figure 3.13: Cumulative energy requirement ASF; EPBT at 7 years

3.1.3 Comparable technologies

The adaptive solar facade acts as a shading system as well as a photovoltaic electricity generation system and is therefore a hybrid system. To benchmark the performance of the ASF in the life cycle assessment, it is compared with both conventional systems individually. First, a comparison with standard louvres is given, whereafter the ASF is compared with standard facade mounted photovoltaic systems.

Shading systems

The ASF is compared with an aluminum static louvres system. This system is made from aluminum alloy at a density of 8kg per square meter of facade. The static louvres system does not require maintenance during its lifetime of 10 years.

From figure 3.14 it can be seen that the ASF requires a significantly larger initial investment in embodied carbon (roughly 3 times larger). However this investment is offset by the extra energy reduction benefits and production of electricity via the solar panels. Also the disposal of the ASF requires more carbon emissions. The end result is that the ASF performs just slightly better than the louvres with a total emissions of negative 51.07 to negative 49.31 respectively.

Although the ASF performs better than the static louvres, a lot depends on the assumptions made in the thesis. For instance, the ASF is assumed to have a lifetime of 15 years, while the result of the static louvres is based on a lifetime of 10 years. Also the country where the ASF is produced, the specifications of the room and country of the building greatly influence the results. The sensitivity analysis, which can be found further on in the thesis, will address these concerns in further detail. Therefore the result that the ASF performs slightly better than the static louvres is only valid for these assumptions and is heavily subject to the exact environment in which both systems operate.

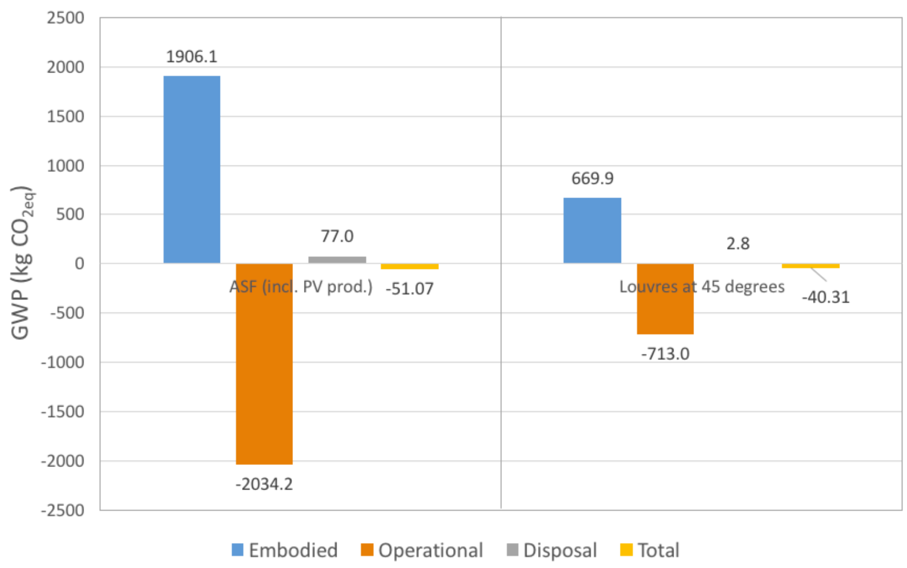

Figure 3.14: GWP comparison for adaptive solar facade and louvres

Photovoltaic building integrated facade systems

The adaptive solar facade is compared with four other static photovoltaic building integrated facade systems: CIGS thin film panels, standard mono silicon panels, standard poly silicon panels and CdTe thin film panels. It is important to note that the ASF is placed in front of a window of a room, while the other facade mounted systems are placed in front of a blind wall. The reason for this is that the ASF is designed to put in front of windows, while the standard photovoltaic building integrated facade systems can only be placed on blind walls. In the comparison all supporting structures are taken into account, especially because the supporting structures of the ASF greatly influence the embodied carbon emissions of the ASF.

Table 3.5 shows the assumptions made for every system. Here, the irradiation and area are the same for every system, as these are location specific and not system specific. At a first glance, it is immediately obvious that the ASF has a much lower performance ratio. This is due to the fact that the actual area of the photovoltaic panels is smaller than 8.96 square meters, furthermore the ASF has self-shading on the panels, which greatly reduces the performance ratio. Other systems have a flat vertical area, hence no self shading occurs.

Also, the lifetime of the thin-film is only 15 years, while standard silicon panels have a lifetime of 20 years. Therefore the electricity production from the ASF and other thin-film technologies is significantly lower than the silicon systems. The lack of performance of the ASF is however compensated in the emissions of the BOS due to energy reductions as a result of shading benefits. The benefits are attributed to the BOS and therefore only have an influence on the total incl. BOS emissions in Table 3.5. The lower emissions from the laminate of the ASF compared to the CIGS system is purely due to the fact that a smaller area of solar panels is used. The ASF uses the same solar panels as the CIGS system, therefore any changes in numbers are inadvertently due to the setup of the ASF compared to the facade mounted system.

Table 3.5: Facade mounted photovoltaic system assumptions, electricity production and carbon emissions comparison

	ASF	**CIGS**	**mono-Si**	**poly-Si**	**CdTe**
Irradiation [kWh/m^2/yr]	1,240	1,240	1,240	1,240	1,240
Efficiency [-]	16.9%	16.9%	16.0%	13.0%	12.0%
Performance ratio [-]	0.22	0.60	0.60	0.60	0.60
Lifetime [yr]	15	15	20	20	15
Area [m^2]	8.96	8.96	8.96	8.96	8.96
PV production [kWh]	**6,255**	**16,899**	**21,331**	**17,332**	**11,999**
Laminate/panel [kg_{CO_2eq}]	674.6	1,000.1	2,451.9	1,866.3	641.2
Total incl. BOS [kg_{CO_2eq}]	793.3	1,103.2	3,005.0	2,397.8	744.3

The exact LCA breakdown of the PV systems used in the calculation can be found in Appendix B.

Figure 3.15 shows the GWP per kWh electricity produced during the lifetime of the systems. It can be seen that the ASF outperforms the silicon systems, however the energy reduction benefits due to shading do not compensate enough for the worse performance ratio of the ASF compared to a CIGS facade mounted system. Similar to the shading system this conclusion highly depends on the assumptions taken, therefore the sensitivity analysis will go into further detail. The use of different assumptions greatly influences the result. Still the ASF performs significantly better than the UCTE mix low voltage average carbon emissions. Therefore installing the

ASF will be greatly beneficial when compared with the UCTE average. The same can be said for all photovoltaic systems, as all systems operate well below 200 grams per kWh produced.

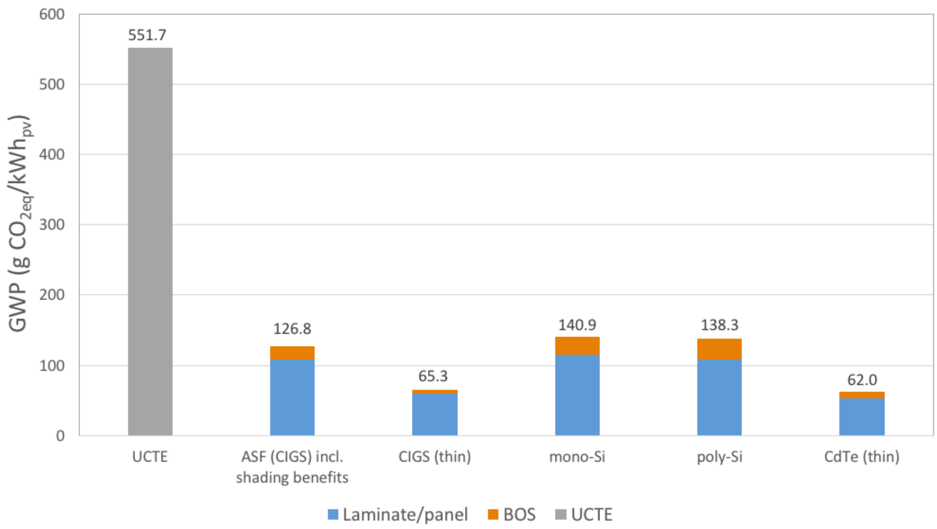

Figure 3.15: Comparison of the ASF with other facade-mounted PV systems

3.1.4 Design considerations

Based on the analyses there are multiple areas where the design can potentially be improved. Both the inventory analysis as the life cycle assessment have shown that the candidates for optimization are mostly the solar panels, the steel frame and the control and electronic systems.

First, the steel frame can be optimized by using interfixing of cables to aviod the need for pretensioning of the cables. Hereby less steel is required for the bars of the frame, reducing the amount chromium steel used.

Second, low-alloyed steel with anti corrosion coating can be used for the frame. Chromium steel 18/18 has a high carbon emissions factor. Therefore changing to a coated low-alloyed steel can reduce carbon emissions.

Third, the panels can be controlled per horizontal row instead of individually. Hereby reductions can be achieved in various sections of the control system:

- amount of 2-2 way valves needed
- length of pneumatic tubes needed
- size of control modules (e.g. NI 9476, NI9205 and NI9403)

Last, the plate area without solar panels can be increased. This will reduce the amount of solar panels used and therefore reduce the embodied carbon emissions. As seen in Figure 3.7, solar panels make up roughly 35 percent of total embodied carbon emissions. This will also help with the self-shading problem of the ASF. Looking at Table 3.5, the PV production is significantly lower than of regular fixed facade mounted systems, using more plate area without solar panels will therefore also make the ASF more efficient in producing electricity (increasing the performance ratio).

3.1.5 Sensitivity analysis

As discussed above, the sensitivity analysis is of great importance to the evaluation of the total carbon emissions of the ASF. Changing assumptions can greatly change the outcome of the LCA result therefore three variabilities will be evaluated in the sensitivity analysis:

- **Operation location**: changing the operation location from Switzerland (carbon emission factor at grid of 135.0 g_{CO_2eq}/kWh) to Germany (carbon emission factor at grid of 671.5 g_{CO_2eq}/kWh)
- **Energy efficiency solar panels**: changing the energy efficiency of the solar panels to inefficient (14.0%) and efficient (18.0%)
- **Room size**: changing the room size behind the ASF to 10 and 30 square meters respectfully.

It is important to note that only one variable will be changed at once, in these scenario's therefore keeping all else equal to the initial assumptions used in the case study. The red line in the Figures 3.16 and 3.17 gives the baseline result from the LCA.

Furthermore, the worst and best case scenario of changing these variables is evaluated (changing all three variables at once). Here the assumptions amplify each other giving the following result:

- **Best case scenario** Germany, energy efficient solar panels and 30 square meters room size: -1115.0 g_{CO_2eq}/kWh and -26.4 kgCO_2/$m^2 * yr$
- **Worst case scenario** Switzerland, energy inefficient solar panels, 10 square meters room size: 298.0 g_{CO_2eq}/kWh and 5.7 kgCO_2/$m^2 * yr$

Figure 3.16 shows that the changing of operation location to Germany has the biggest impact. The result goes from 126.8 g_{CO_2eq}/kWh to -762.0 g_{CO_2eq}/kWh. The reason for this is that the emission factor of electricity at the grid is roughly 5 times higher in Germany compared to Switzerland. Therefore the carbon emissions reduction due to energy savings in heating, lighting and cooling also gets magnified by a factor 5. Looking back at Figure 3.9 this then gives a total carbon emission during the lifetime of the ASF excluding PV production of -4766.3 kg_{CO_2eq}.

Second, it can be seen that the energy efficiency difference only has a small impact, this is due to the fact that only a different electricity production is used to divide the total emissions with, therefore having a small impact ranging from 119.1 g_{CO_2eq}/kWh to 153.1 g_{CO_2eq}/kWh.

Third, the room size also has an impact on carbon emission reductions due to energy savings in heating, lighting and cooling. As only the energy requirement of the room is changed and not the emission factor, it has an impact which is bigger than the impact of the solar panel efficiency, but smaller than the impact of the operation location. The range goes from 41.4 g_{CO_2eq}/kWh to 247.5 g_{CO_2eq}/kWh respectively.

Last, the best and worst case scenario shows the total amplification of combined variable changes. The best case scenario is actually not the overall best case scenario for this metric of g_{CO_2eq}/kWh. The reason for this is that the best case scenario has a negative result, therefore it would be better to have as inefficient solar panels as possible to get the best case scenario for this metric. As also the other metric of $kgCO_2eq/m^2 * yr$ is used however, the best case scenario is kept as described above, as for the metric per square meter per year most efficient solar panels would be better. The range goes from -1115.0 g_{CO_2eq}/kWh to 298 g_{CO_2eq}/kWh respectively.

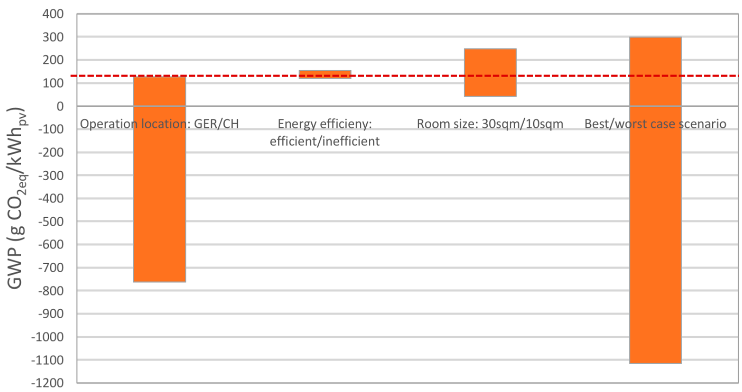

Figure 3.16: Sensitivity analysis based on gCO_2eq/kWh_{pv}

Figure 3.17 shows that the changing of operation location to Germany has the biggest impact. The result goes from -27.5 $kgCO_2eq/m^2 * yr$ to -0.2 $kgCO_2eq/m^2 * yr$. The reason for this is that the emission factor of electricity at the grid is again roughly 5 times higher in Germany compared to Switzerland. Therefore the carbon emissions reduction due to energy savings in heating, lighting and cooling also gets magnified by a factor 5. Looking back at Figure 3.9 this then gives a total carbon emission during the lifetime of the ASF including PV production of -8951.3 kg_{CO_2eq}.

Second, it can be seen that the energy efficiency difference only has a large impact. This is due to the fact that more or less electricity production directly translates into a difference in total emissions of the ASF including PV production. Therefore the impact ranges from -4.9 $kgCO_2eq/m^2 * yr$ to 4.3 $kgCO_2eq/m^2 * yr$.

Third, the room size also has an impact on carbon emission reductions due to energy savings in heating, lighting and cooling and the division by room size and year of operation. As both the energy requirement of the room and division by room size are changed, but not the emission factor, it has an impact which is smaller than both the impact of the solar panel efficiency and the impact of the operation location. Furthermore because the number of room size of 30 square meters is negative (-585 kg_{CO_2eq}), the result is damped by the larger room due to division. The resulting range is -1.3 $kgCO_2eq/m^2 * yr$ to 4.7 $kgCO_2eq/m^2 * yr$.

Last, the best and worst case scenario shows the total amplification of combined variable changes. The best case scenario is actually not the overall best case scenario for this metric of $kgCO_2eq/m^2 * yr$. The reason for this is that the best case scenario has a negative result, therefore it would be better to have an as small room as possible to get the best case scenario for this metric. As also the other metric of gCO_2eq/kWh_{pv} is used however, the best case scenario is kept as described above, as for the metric per kWh a bigger room would be better. Therefore the impact ranges from -26.4 $kgCO_2eq/m^2 * yr$ to 5.7 $kgCO_2eq/m^2 * yr$.

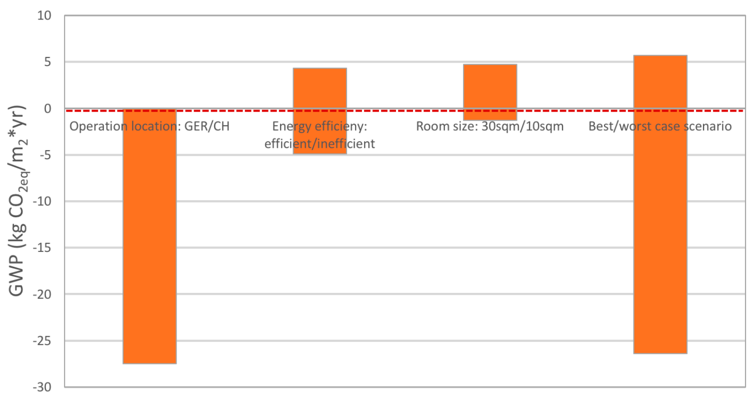

Figure 3.17: Sensitivity analysis based on $kgCO_2eq/m^2 * yr$

3.1.6 Monte-carlo simulation

The sensitivity analysis section has focused on the operational assumptions e.g. location, room size and efficiency of solar panels. Next, a monte-carlo simulation is performed on the embodied carbon emissions calculation of the ASF to get a full picture on uncertainties in all aspects of the life cycle assessment. Quantaties of materials used in the ASF also have uncertainties, just like the operational assumptions. As quantities in a production process mostly have a normal distribution, a monte-carlo simulation would fit best to evaluate this uncertainty range.

A lognormal distribution for quantities is used based on the Ecoinvent database assumptions for all processes.

3.2 Case study II: Funicular floor

The case study for the funicular floor is developed for the Hilo building unit to be constructed for the NEST project in partnership with EMPA and EAWAG in Dubendorf, Switzerland. The total floor area of the building is 371m^2. Figure 3.18 shows the geometry of these floor slabs. In Appendix C it can be seen that these floor slabs are only used in a small portion of the total 371m^2, namely the bedrooms and bathrooms only.

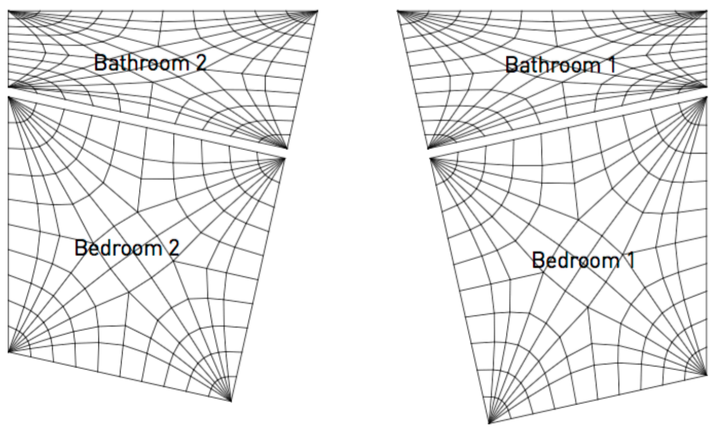

Figure 3.18: Geometry of the four floor slabs including rib patterns[93]

The funicular floor is an extremely lightweight concrete floor slab, reducing the weight by 70 percent compared to a normal concrete prefabricated floor slab[93]. It uses properties of thin-shell funicular vaulting, e.g. large surface area with low material volume to achieve the weight reduction.

3.2.1 Overview

Technical description

The funicular floor is built up out of several layers and has a variable cross section thickness. The floor has five layers, as also can be seen in Figure 3.20:

- Three-ply core plywood finishing floor with fixed thickness
- Impact sound insulation layer with fixed thickness
- Structural plywood layer with fixed thickness
- Expanded polystyrene within the gaps in the concrete funicular structure
- Concrete funicular structure with a variable shape

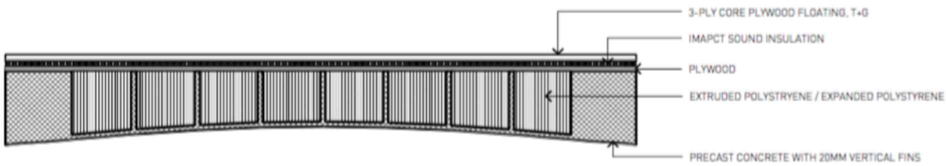

Figure 3.19: Schematic drawing of the floor slab build-up layers[93]

Furthermore steel tension ties at the perimeter of the floor slab used for post-tensioning. The funicular floor is constructed using a plywood box as mold, where the lower curvature is created by a milled polystyrene block. The gaps in the concrete are created by milled polystyrene shapes, which are inserted before the concrete is poured into the mold.

Figure 3.20: Upper and lower sections of the mold including concrete slab[93]

Flow diagram

Inventory analysis

Table 3.6: Technical description of the funicular floor

Material description	τ [mm]	V [m^3/m^2]	ρ [kg/m^3]	SMQ [kg/m^2]
Plywood, for indoor use	27	0.02700	540	14.58
Polyurethane, rigid foam	20	0.02000	500	10.00
Plywood, for indoor use	18	0.01800	540	9.72
Polystyrene, expanded [a]	var	0.08740	30	2.62
Concrete, 50MPa	var	0.05779	2,328	134.56
Steel, low alloyed[b]	NA	?	?	?

[a]Milled blocks between concrete; 0.86m^3 for a 9.84m^2 area
[b]Rings for post-tensioning

Table 3.7: Technical description of the supporting structures and processes

Material description	τ [mm]	V [m^3/m^2]	ρ [kg/m^3]	SMQ [kg/m^2]
Polystyrene, expanded[a]	var.	0.08740	30	2.62
Plywood, for indoor use[b]	?	?	540	?
Lorry, >32t, EURO6[c]	NA	NA	NA	?

[a]Lower section of mold only; 0.86m^3 for a 9.84m^2 area
[b]Upper and lower case of the mold
[c]Based on an average of 100 km point-to-point and total mass of funicular floor including supporting structures and processes

3.2.2 Life cycle assessment

3.2.3 Comparable technologies

3.2.4 Design considerations

3.2.5 Sensitivity analysis

3.3 Case study III: Thin-shell roof

Figure 3.21: [93]

3.3.1 Overview

Technical description

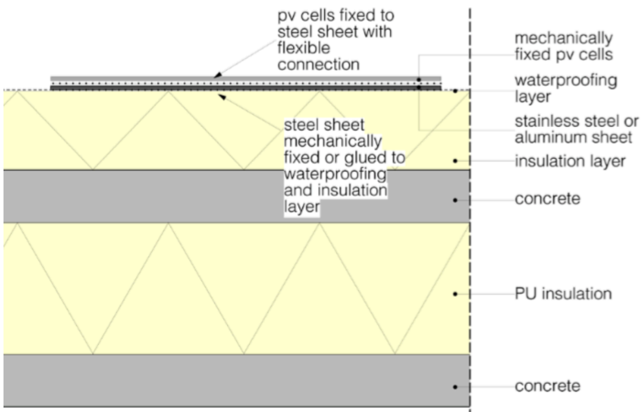

Figure 3.22: [93]

Flow diagram

Inventory

-371m^2 floor area
-157m^2 roof area
-ratio: 0.423180593

Table 3.8: Technical description of the thin-shell roof

Material description	τ [mm]	V [m^3/m^2_{floor}]	ρ [kg/m^3]	SMQ [kg/m^2_{floor}]
CIGS thin film[a]	?	?	?	?
Chromium steel, hot rolled [b]	?	?	?	?
Polyurethane, rigid foam	41	0.01735	500	8.68
Concrete, normal	37	0.01566	2,380	37.27
AR Glass-fibre[c]	var	0.00036	2,700	0.96
Polyurethane, rigid foam	68	0.02878	500	14.39
Concrete, normal	37	0.01566	2,380	37.27
Steel, B500A[d]	var	0.00156	7,850	12.27
Concrete, normal	10	0.00423	2,380	10.07

[a]Total of x m^2
[b]Total of x m^2 at x mm
[c]1% of total volume concrete
[d]B500A reinforcing mesh; absolute volume of 0.58 m^3/m^2_{floor}

Table 3.9: Technical description of the supporting structures and processes

Material description	τ [mm]	V [m^3/m^2_{floor}]	ρ [kg/m^3]	SMQ [kg/m^2_{floor}]
Glulam timber, indoor use[a]	NA	0.02833	450	12.75
Steel, low alloyed[b]	NA	0.00045	8,000	3.61
Steel, low alloyed[c]	NA	0.00013	8,000	1.01
Polypropylene, granulate[d]	55	0.02833	946	26.80
Plywood, outdoor use[e]	27	0.01077	540	5.82
Lorry, >32t, EURO6[f]	NA	NA	NA	?

[a]Glued, laminated beams 80x300mm at length of 438m
[b]Tubular steel frame S235 RO 273/2.6 at length of 75m
[c]Steel cable, 8mm diameter at length of 936m
[d]Fabric at 157m^2 + 20% waste; hence a total of 188.4m^2
[e]Plating and strengthening of the supporting frame at 148m^2
[f]Based on an average of 100 km point-to-point and total mass of thin-shell roof including supporting structures

3.3.2 Life cycle assessment

3.3.3 Comparable technologies

3.3.4 Design considerations

3.3.5 Sensitivity analysis

Chapter 4

Closure

4.1 Conclusion

4.2 Discussion

Importance of country for ASF....

Didn't include supporting structure of the building impact floor slab!

4.3 Outlook

Appendix A

Disposal processes

Table A.1: Disposal datasets Ecoinvent for the Adaptive Solar Facade

Material type	Disposal process
Steel	Treatment of waste scrap steel
Aluminum	Treatment of waste scrap aluminum
Copper	Treatment of waste scrap copper
PV cables	Treatment of waste electric wiring
Internet cable	Treatment of waste electric wiring
Polyethylene	Treatment of waste polyethylene
Polyvinylchloride	Treatment of waste polyvinylchloride
2-2 way valve	Electronics scrap from control units
c-Rio 9066, 8-slot, integrated 667MHz	Electronics scrap from control units
NI9205 32ch AI with cables and connectors	Electronics scrap from control units
NI9403 32ch 5V-TTL bidirectional DI-O	Electronics scrap from control units
NI9476 32ch DO with cables and connectors	Electronics scrap from control units
Inverter	Waste electric and electronic equipment
Voltage regulator	Waste electric and electronic equipment
Bypass diode	Waste electric and electronic equipment
Rubber	Treatment of waste rubber
CIGS film	Treatment of residual material landfill
Polyurethane	Treatment of waste polyurethane
All residual material	Treatment of residual material landfill

Appendix B

Breakdown of PV systems

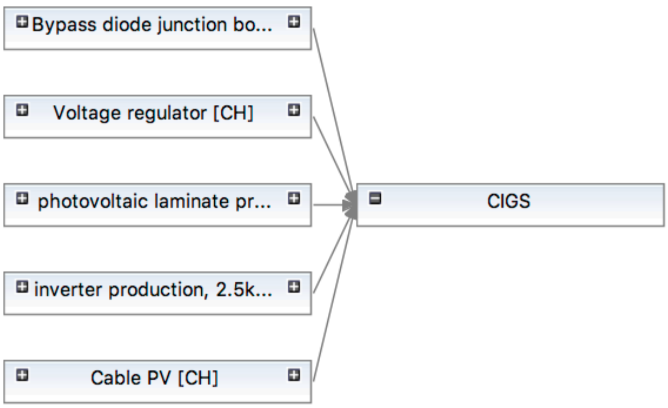

Figure B.1: Breakdown CIGS thin-film facade system

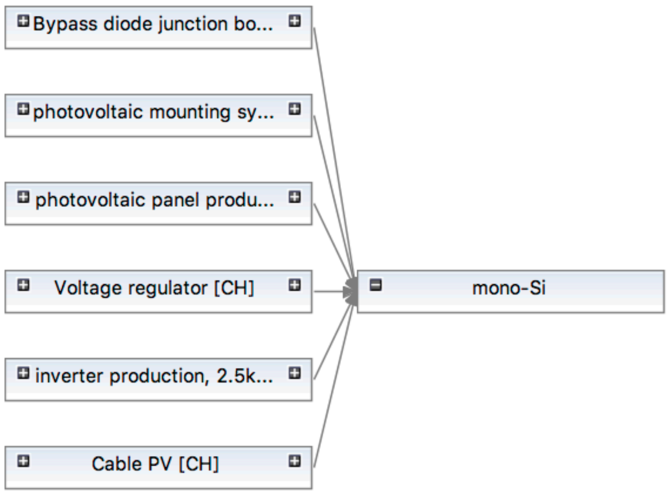

Figure B.2: Breakdown mono-Si facade system

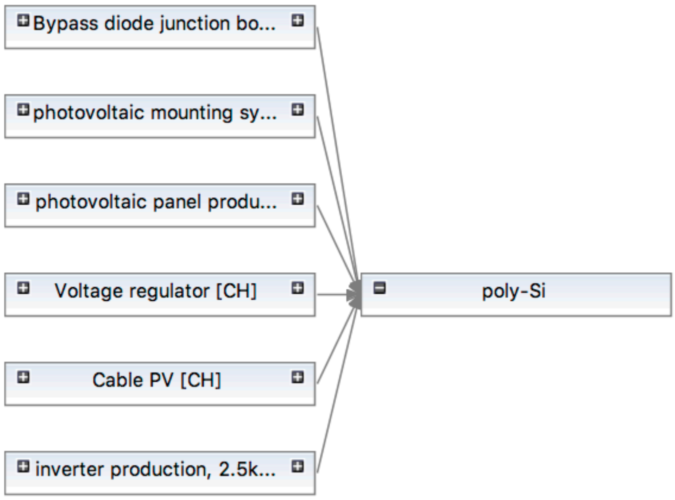

Figure B.3: Breakdown poly-Si facade system

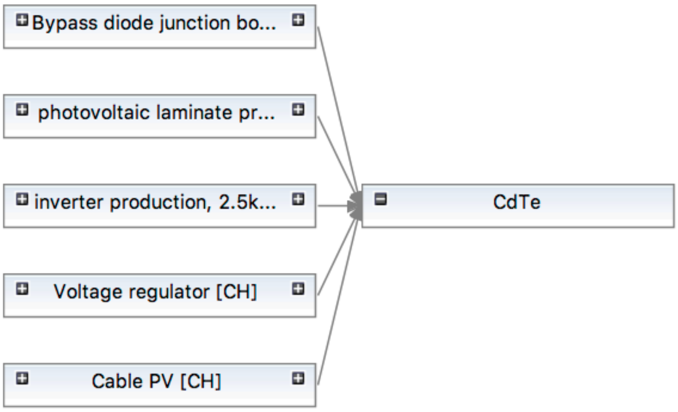

Figure B.4: Breakdown CdTe thin-film facade system

Appendix C

Detailed product information and results

Figure C.1: Three technologies schematic overview and interdependence: roof, floor and adaptive solar facade[93]

C.1 Detailed inventory analysis

C.1.1 Adaptive Solar Facade

Describe all processes and quantities...

C.1.2 Funicular floor

Describe all processes and quantities...

C.1.3 Thin-shell roof

Describe all processes and quantities...

C.2 Detailed results

...

▼100.00%	ASF A - CH	1906.14577	kg CO2-Eq
▼35.39%	Solar panel - CH	674.57941	kg CO2-Eq
▶27.92%	PV film flisom - CH	532.17751	kg CO2-Eq
▶07.32%	Aluminum sheet for PV film - CH	139.48688	kg CO2-Eq
▶00.15%	Glue 2 comp - CH	2.91502	kg CO2-Eq
▼23.84%	Control and electronic systems - CH	454.39047	kg CO2-Eq
▶07.05%	Air compressor - CH	134.37782	kg CO2-Eq
▶05.66%	Inverter - CH	107.87196	kg CO2-Eq
▶04.56%	Cable PV - CH	86.85917	kg CO2-Eq
▶02.10%	2-2 way valve - CH	39.96447	kg CO2-Eq
▶01.85%	Bypass diode junction box - CH	35.21262	kg CO2-Eq
▶00.92%	c-Rio 9066, 8-slot, integrated 667Mhz - CH	17.53262	kg CO2-Eq
▶00.31%	Internet cable - CH	5.92094	kg CO2-Eq
▶00.26%	Voltage regulator - CH	4.95427	kg CO2-Eq
▶00.23%	Manifold block - CH	4.37790	kg CO2-Eq
▶00.23%	NI 9205 32ch AI with cables and connect...	4.34875	kg CO2-Eq
▶00.22%	NI 9403 32ch 5V-TTL bidirectional DI-O...	4.12856	kg CO2-Eq
▶00.21%	Cable for the valves - CH	4.09659	kg CO2-Eq
▶00.21%	NI 9476 32ch DO with cables and conne...	4.04599	kg CO2-Eq
▶00.04%	M3 plugin connector - CH	0.69880	kg CO2-Eq
▼21.33%	Steel frame - CH	406.51234	kg CO2-Eq
▶11.12%	Steel bar L profile - CH	212.00644	kg CO2-Eq
▶09.18%	Steel bar U profile - CH	175.02224	kg CO2-Eq
▶00.54%	Swaged external thread - CH	10.33940	kg CO2-Eq
▶00.33%	Steel wire rope WC - CH	6.26065	kg CO2-Eq
▶00.06%	Post fitting for external thread - CH	1.16209	kg CO2-Eq
▶00.04%	Adjustable cross clamp - CH	0.72590	kg CO2-Eq
▶00.03%	chromium steel drilling, conventional - RER	0.64612	kg CO2-Eq
▶00.01%	Bolt - CH	0.25595	kg CO2-Eq
▶00.00%	Nut - CH	0.07313	kg CO2-Eq
▶00.00%	Washer - CH	0.02043	kg CO2-Eq
▼13.18%	Actuator - CH	251.18288	kg CO2-Eq
▶03.99%	Panel adapter - CH	76.10025	kg CO2-Eq
▶03.64%	Tubes - CH	69.29908	kg CO2-Eq
▶03.43%	Steel ring - CH	65.28819	kg CO2-Eq
▶01.49%	Silicone chamber - CH	28.48634	kg CO2-Eq
00.24%	Bolt - CH	4.60702	kg CO2-Eq
▶00.14%	Mold for actuator - CH	2.64523	kg CO2-Eq
00.07%	Nut - CH	1.31629	kg CO2-Eq
00.06%	Glue 2 comp - CH	1.20973	kg CO2-Eq
▶00.05%	Hose connector type GRS - CH	0.90955	kg CO2-Eq
▶00.03%	Baking actuator - CH	0.63561	kg CO2-Eq
00.02%	Washer - CH	0.36779	kg CO2-Eq
▶00.02%	Vacuuming actuator - CH	0.31780	kg CO2-Eq
▼04.34%	Cantilever bracket - CH	82.63837	kg CO2-Eq
▶03.99%	Steel bracket - CH	76.10025	kg CO2-Eq
00.24%	Bolt - CH	4.60702	kg CO2-Eq
▶00.10%	Fixing clamp - CH	1.93111	kg CO2-Eq
▼01.93%	Assembling ASF - CH	36.84231	kg CO2-Eq
▶01.93%	market for machine operation, diesel, < 1...	36.84231	kg CO2-Eq

Figure C.2: Embodied GWP contribution tree of the ASF

Bibliography

[1] I. Sartori and A. Hestnes, "Energy use in the life cycle of conventional and low energy buildings: a review," *Energy and Buildings*, 2007.

[2] L. Aye, T. Ngo, R. Crawford, R. Gammampila, and P. Medis, "Life cycle greenhouse gas emissions and energy analysis of prefrabricated reusable building modules," *Energy and Buildings*, vol. 47, pp. 159–168, 2012.

[3] C. de Wolf, "Material quantities in building structures and their environmental impact," Master's thesis, Massachusetts Institute of Technology, 2014.

[4] [Online]. Available: https://www.ethz.ch/en/news-and-events/eth-news/news/2015/06/soft-robotics-for-adaptive-building-facades/_jcr_content/news_content/fullwidthimage/image.imageformat.lightbox.2057198173.png

[5] thin-shell roof. [Online]. Available: http://hilo.arch.ethz.ch/?page_id=84

[6] *The New International Standards for Life Cycle Assessment: ISO 14040 and ISO 14044*, International Organization for Standardization Std., 2006.

[7] G. Hammond and C. Jones, "Embodied energy and carbon in construction materials," in *Proceedings of the Institution of Civil Engineers*, vol. 161, 2008, pp. 87–98.

[8] M. Raugei, S. Bargigli, and S. Ulgiati, "Life cycle assessment and energy pay-back time of advanced photovoltaic modules: Cdte and cis compared to poly-si," *Energy*, vol. 32, pp. 1310–1318, 2007.

[9] J. Sjunnesson, "Life cycle assessment of concrete," Master's thesis, Lund University, 2005.

[10] [Online]. Available: http://www.ecoinvent.org/database/ecoinvent-version-3/system-models-in-ecoinvent-3/cut-off-system-model/allocation-cut-off-by-classification.html

[11] R. Frischknecht and M. Stucki, "Life cycle inventories of electricity mixes and grid," Paul Scherrer Institut, Tech. Rep., 2014.

[12] R. Speck, S. Selke, R. Auras, and J. Fitzsimmons, "Life cycle assessment software: selection can impact results," *Journal of Industrial Ecology*, 2015.

[13] ReCiPe. [Online]. Available: http://www.lcia-recipe.net/_/rsrc/1332430005250/project-definition/ReCiPe_overview.png

[14] P. Jayathissa, "Numerical simulation of energy performance and construction of the adaptive solar facade," in *Advanced Building Skins Conference*, 2015.

[15] Flisom. Roll-to-roll (r2r) manufacturing process. [Online]. Available: http://www.flisom.com/technology.php#rolltoroll

[16] O. Ortiz, F. Castells, and G. Sonnemann, "Sustainability in the construction industry: A review of recent developments based on lca," *Construction and building materials*, vol. 23, pp. 28–39, 2009.

[17] R. de Groot, M. Wilson, and R. Boumans, "A typology for the classification, description and valuation of ecosystem functions, goods and services," *Ecological Economics*, vol. 41, pp. 393–408, 2002.

[18] A. Sherwani, J. Usmani, and Varun, "Life cycle assessment of solar pv based electricity generation systems: A review," *Renewable and Sustainable Energy Reviews*, vol. 14, pp. 540–544, 2010.

[19] A. Stoppato, "Life cycle assessment of photovoltaic electricity generation," *Energy*, vol. 33, pp. 224–232, 2008.

[20] O. Edenhofer, R. PichsMadruga, and Y. Sokona, "Fifth assessment report," Intergovernmental Panel on Climate Change, Tech. Rep., 2014.

[21] P. Huovila, "Buildings and climate change: status, challenges and opportunities," *United Nations Environment Program. Sustainable Consumption and Reduction Branch*, 2007.

[22] J. Ochsendorf, "Challenges and opportunities for low-carbon buildings," *The Bridge*, vol. 42, pp. 26–32, 2012.

[23] S. Pacala and R. Socolow, "Stabilization wedges: solving the climate problem for the next 50 years with current technologies," *Science*, vol. 305, pp. 968–972, 2004.

[24] (2009) Transforming the market: Energy efficiency in buildings. World Business Council for Sustainable Development. [Online]. Available: http://www.wbcsd.org/Pages/EDocument/EDocumentDetails.aspx?ID=11006

[25] P. Enkvist, T. Nauclér, and J. Rosander, "A cost curve for greenhouse gas reduction," *McKinsey Quarterly*, 2007.

[26] C. JimenezGonzalez, D. J. C. Constable, and C. S. Ponder, "Evaluating the greenness of chemical processes and products in the pharmaceutical industry: a green metrics primer," *Chemical Society Reviews*, vol. 41, pp. 1485–1498, 2012.

[27] D. Constable, A. Curzons, and V. Cunningham, "So you think your process is green how do you know: Using principles of sustainability to determine what is green: a corporate perspective," *Green Chemistry*, vol. 4, pp. 521–527, 2002.

[28] B. Ridoutt, P. Fantke, S. Pfister, J. Bare, A. Boulay, F. Cherubini, R. Frischknecht, M. Hauschild, and S. Hellweg, "Previous article next article table of contents making sense of the minefield of footprint indicators," *Environmental Science and Technology*, vol. 49, pp. 2601–2603, 2015.

[29] H. de Bruijn, R. van Duin, and M. A. J. Huijbregts, *Handbook on Life Cycle Assessment*, J. Guinee, M. Gorree, R. Heijungs, and G. Huppes, Eds. Springer, 2002.

[30] S. Hellweg and L. Canals, "Emerging approaches, challenges and opportunities in life cycle assessment," *Science*, vol. 344, pp. 1109–1113, 2014.

[31] C. Scheuer, G. Keoleian, and P. Reppe, "Life cycle energy and environmental performance of a new university building: modeling challenges and design implications," *Energy and Buildings*, vol. 35, pp. 1049–1064, 2003.

[32] K. Eaton and A. Amato, "A comparative life cycle assessment of steel and concrete framed office buildings," *Journal of Constructional Steel Research*, vol. 46, pp. 286–287, 1998.

[33] L. Cabeza, L. Rincon, V. Vilarino, G. Perez, and A. Castell, "Life cycle assessment (lca) and life cycle energy analysis (lcea) of buildings and the building sector: A review," *Renewable and Sustainable Energy Reviews*, vol. 29, pp. 394–416, 2014.

[34] D. Saner, N. Heeren, B. Jaggi, R. Waraich, and S. Hellweg, "Housing and mobility demands of individual households and their life cycle assessment," *Environmental Science and Technology*, vol. 47, pp. 5988–5997, 2013.

[35] S. Pauliuk, K. Sjostrand, and D. Muller, “Transforming the norwegian dwelling stock to reach the 2 degrees celsius climate target,” *Journal of Industrial Ecology*, vol. 17, pp. 542–554, 2013.

[36] J. Guinee, R. Heijungs, G. Huppes, A. Zamagni, P. Masoni, R. Buonamici, and T. Ekvall, “Life cycle assessment: past, present and future,” *Environmental Science and Technology*, vol. 45, pp. 90–96, 2011.

[37] T. Swarr, D. Hunkeler, W. Klopffer, H. Pesonen, and A. Ciroth, “Environmental life-cycle costing: a code of practice,” *International Journal of Life Cycle Assessment*, vol. 16, pp. 389–391, 2011.

[38] A. Levasseur, P. Lesage, M. Margni, L. Deschenes, and R. Samson, “Considering time in lca: Dynamic lca and its application to global warming impact assessments,” *Environmental Science and Technology*, vol. 44, pp. 3169–3174, 2010.

[39] M. Dixit, J. Solis, S. Lavy, and C. Culp, “Need for an emodied energy measurement protocal for buildings: A review paper,” *Renewable and Sustainable Energy Reviews*, vol. 16, pp. 3730–3743, 2012.

[40] S. Kaethner and J. Burridge, “Embodied co2 of structural frames,” *The Structural Engineer*, pp. 33–40, May 2012.

[41] K. Adalberth, “Energy use during the life cycle of buildings: a method,” *Building and Environment*, vol. 4, pp. 317–320, 1999.

[42] R. Cole and P. Kernan, “Life-cycle energy use in office buildings,” *Building and Environment*, vol. 4, pp. 307–317, 1996.

[43] M. Webster, H. Meryman, A. Slivers, T. Rodriguez, L. Lemay, and K. Simonen, “Strucutre and carbon: How materials affect the climate,” in *SEI Sustainability Committee, Carbon Working Group*, 2012.

[44] C. Thormark, “A low energy building in a life cycle its embodied energy, energy need for operation and recycling potential,” *Building and Environment*, vol. 4, pp. 249–455, 2002.

[45] Reddy and Jagadish, “Embodied energy of common and alternative building materials and technologies,” *Energy and Buildings*, vol. 2, no. 129-137, 2003.

[46] S. Simpson, F. Cousins, E. Ayaz, and F. Yang, “Zero carbon is not really zero: why embodied carbon in materials cannot be ignored,” *Design Intelligence*, 2010.

[47] (2013, December) Estimate the embodied co2 of a whole construction project. Build Carbon Neutral. [Online]. Available: http://buildcarbonneutral.org

[48] (2009) Impact estimator for buildings. Athena Sustainable Material Institute. [Online]. Available: http://www.athenasmi.org

[49] Arup, "Structural scheme design guide," Arup, Tech. Rep., 2008.

[50] A. Lenoir, S. Cory, M. Donn, and F. Garde, "Optimisation methomethod for the design of solar shading for thermal and visual comfort in tropical climates," in *13th Conference of International Buidling Performance Simulation Association*, 2013.

[51] P. Marrero, I. Ana, and O. Armando, "Effecit of lower shaing devices on building energy requirements," *Applied Energy*, vol. 87, pp. 2040–2049, 2010.

[52] A. Almussaed and A. Almssad, "Natural lighting efficiency by means of sun-skylight tubues," *International Journal of Engineering and Advanced Technology*, vol. 3.

[53] M. Santamouris, A. Synnefa, D. Kolokotsa, V. Dimitriou, and K. Apostolakis, "Passive cooling of the built environment: use of innvovative reflective materials to fight heat islands and decrease cooling needs," *International Journal of Low Carbon Technologies*, vol. 3, 2008.

[54] J. Rizk and Y. Chaiko, "Solar tracking system: more efficient use of solar," *World Academy of Science, Engineering and Technology*, vol. 3, 2008.

[55] B. Svetozarevic, Z. Nagy, D. Rossi, and A. Schlueter, "Experimental characterization of a 2 dof soft robotic platform for architectural applications."

[56] R. Fortmeyer and C. Linn, "Kinetic architecture: designs for active envelopes," in *Images publishing*, 2014.

[57] E. Giselbrecht, "Dynamic facades," in *Advanced Building Skins, Gratz, Austria*, 2012.

[58] D. Veenendaal, J. Bakker, and P. Block, "Structural design of the cable-net and fabric formed, ferrocement sandwich shell roof of nest hilo," *Proceedings of the International Association for Shell and Spatial Structures*, 2015.

[59] D. Lopez, D. Veenendaal, M. Akbarzadeh, and P. Block, "Prototype of an ultra-thin, concrete vaulted floor system," in *Proceedings of the IASS-SLTE 2014 Symposium*, 2014.

[60] K. Adalberth, A. Almgren, and E. Petersen, "Life cycle assessment of four multi family buildings," *International Journal for Low Energy Sustainable Buildings*, 2001.

[61] F. Ardente, “Life cycle assessment of a solar thermal collector,” *Renewable Energy*, vol. 30, pp. 1031–1054, 2005.

[62] A. Arena and C. Rosa, “Life cycle assessment of energy and environmental implications of the implementation of conservation technologies in school buildings in mendoza,” *Building Environment*, vol. 38, pp. 359–368, 2003.

[63] M. Asif, T. Muneer, and R. Kelley, “Life cycle assessment: a case study of a dwelling home in scotland,” *Building Environment*, vol. 11, 2005.

[64] S. Citherlet, F. Guglielmo, and J. Gay, “Window and advanced glazing systems life cycle assessment,” *Energy Buildings*, vol. 32, pp. 225–234, 2000.

[65] G. Jian, L. Jiang, and H. Kazuroni, “Life cycle assessment in the environmental impact evaluation of urban development: a case study of land readjustment project,” *Journal of Zheijiang University of Science*, vol. 4, pp. 702–708, 2003.

[66] S. Junnila, “Life cycle assessment of environmentally significant aspects of an office building,” *Nordic Journal Surveying Real Estate*, 2004.

[67] C. Koroneos and A. Dompros, “Environmental assessment of brick production in greece,” *Building Environment*, vol. 42, pp. 2114–2123, 2006.

[68] C. Koroneos and G. Kottas, “Energy consumption modeling analysis and environmental impact assessment of model house in thessaloniki greece,” *Building Environment*, vol. 42, pp. 122–138, 2007.

[69] B. Nebel, B. Zimmer, and G. Wegener, “Life cycle assessment of wood floor coverings: a representative study for the german flooring industry,” *International Journal of Life Cycle Assessment*, vol. 11, pp. 172–182, 2006.

[70] G. Nicoletti, B. Notarnicola, and G. Tassielli, “Comparative life cycle assessment of flooring materials: ceramic versus marble tiles,” *Journal Cleaner Production*, vol. 10, pp. 283–296, 2002.

[71] M. Nyman and C. Simonson, “Life cycle assessment of residential ventilation units in a cold climate,” *Building Environment*, vol. 40, pp. 15–27, 2005.

[72] B. Peuportier, “Life cycle assessment applied to the comparative evaluation of single family houses in the french context,” *Energy Buildings*, vol. 33, pp. 443–450, 2001.

[73] A. Petersen and B. Solberg, "Environmental and economic iimpact of substitution between wood products and alternative materials: a review of microlevel analyses from norway and sweden," *Forrest Policy Economics*, vol. 7, pp. 249–259, 2005.

[74] M. Prek, "Environmental impact and life cycle assessment of heating and air conditioning systems, a simplified case study," *Energy Buildings*, vol. 36, pp. 1021–1027, 2004.

[75] S. Ross and D. Evans, "The environmental effect of reusing and recycling a plastic-based packaging system," *Journal of Cleaner Production*, vol. 11, pp. 561–571, 2003.

[76] S. Saiz, "Comparative life cycle assessment of standard and green roofs," *Environmental Science and Technology*, vol. 40, pp. 4312–4316, 2006.

[77] L. Schleisner, "Life cycle assessment of a wind farm and related externalities," *Renewable Energy*, vol. 20, pp. 279–288, 2000.

[78] J. Seppala, "The finnish metals industry and the environment," *Resource Conservative Recycling*, vol. 35, pp. 61–76, 2002.

[79] X. Wu, Z. Zhang, and Y. Chen, "Study of the environmental impacts based on the green tax applied to several types of building materials," *Building Environment*, vol. 40, pp. 227–237, 2005.

[80] S. Lizin, S. Passel, E. Schepper, W. Maes, L. Lutsen, J. Manca, and D. Vanderzande, "Life cycle analyses of organic pphotovoltaics: a review," *Energy & Environmental Science*, vol. 6, pp. 3136–3149, 2013.

[81] W. Dias and S. Pooliyadda, "Quality based energy contents and carbon coefficients for building materials: A systems approach," *Energy*, vol. 29, pp. 561–580, 2004.

[82] W. Braham and J. Hale, *Rethinking Technology: A reader in Architectural theory.* Routledge, 2013.

[83] M. Ali and K. Moon, "Structural developments in tall buildings: Current trends and future prospects," *Architectural Science Review*, vol. 50, pp. 205–223, 2007.

[84] A. Alcorn, "Embodied energy coefficients of building materials," in *Centre for Building Performance Research, Victoria University of Wellington*, 1996.

[85] E. Alsema, D. Frail, R. Frischknecht, and M. Held, "Methodology guidelines on life cycle assessment of photovoltaic electricity," *LCA*, 2009.

[86] H. Kim, V. Fthenakis, J. Choi, and D. Turney, "Life cycle greenhouse gas emissions of thin-film photovoltaic electricity generation," *journal of Industrial Ecology*, vol. 16, no. S1, 2012.

[87] A. Moncaster and K. Symons, "A method and tool for cradle to grave embodied carbon and energy impacts of uk buildings in compliance with the new tc350 standards," *Energy and Buildings*, vol. 66, pp. 514–523, 2013.

[88] PECD, "Project embodied carbon database," Arup, Tech. Rep., 2013.

[89] Ecoinvent. (2015) Ecoinvent. Swuss Centre for Life Cycle Inventories. [Online]. Available: http://www.ecoinvent.ch

[90] (2013) Gabi lva database. GaBi. [Online]. Available: www.gabi-software.com

[91] J. Schumaker. (2014) Embodied carbon efficiency tool. Thornton Tomasetti. [Online]. Available: www.thorntontomasetti.com

[92] (2015) Us life cycle inventory database. NREL. [Online]. Available: http://www.nrel.gov/lci/

[93] P. Block and A. Schlueter, "Hilo; ultra-lightweight construction with novel building systems integration," ETH Zurich, Tech. Rep., 2015.